NAVAL SHIP RESEARCH AND DEVELOPMENT CENTER
Washington, D.C. 20007

VENTILATION, CAVITATION AND OTHER CHARACTERISTICS OF HIGH SPEED SURFACE-PIERCING STRUTS

by

Richard S. Rothblum
Dennis A. Mayer
and
Gene M. Wilburn

HYDROMECHANICS LABORATORY
RESEARCH AND DEVELOPMENT REPORT

July 1969

Report 3023

VENTILATION, CAVITATION AND OTHER CHARACTERISTICS OF HIGH SPEED SURFACE-PIERCING STRUTS

The Naval Ship Research and Development Center is a U.S. Navy center for laboratory effort directed at achieving improved sea and air vehicles. It was formed in March 1967 by merging the David Taylor Model Basin at Carderock, Maryland and the Marine Engineering Laboratory at Annapolis, Maryland. The Mine Defense Laboratory, Panama City, Florida became part of the Center in November 1967.

Naval Ship Research and Development Center
Washington, D.C. 20007

NDW-NSRDC 3960/43 (10-67)

DEPARTMENTOFTHE NAVY

NAVAL SHIP RESEARCH AND DEVELOPMENT CENTER

WASHINGTON, D. C. 20007

VENTILATION, CAVITATION AND OTHER CHARACTERISTICS OF HIGH SPEED SURFACE-PIERCING STRUTS

by

Richard S. Rothblum
Dennis A. Mayer
and
Gene ht. Wilburn

July 1969 Report 3023

TABLEOFCONTENTS

LIST OF FIGURES

ABSTRACT

A family of five struts was towed to pierce the water surface vertically in the high-speed towing tank of the Naval Ship Research and Development Center. The purpose of the tests was to determine the effect of speed and certain geometric parameters on the ventilation, cavitation, and other hydrodynamic characteristics of surface-piercing struts.

It was found that upon ventilation at high speeds, significant reversal of side forces may occur on surface-piercing struts. For initially undisturbed conditions, ventilation at high speeds is most likely to occur on blunt-nosed struts. Cavitation results in unpredictable, nonlinear, and highly unsteady force coefficients. Mean force coefficients are presented for the conditions tested. There was some indication that modeling of ventilation inception conditions may be accomplished if Froude and cavitation number are scaled.

ADMINISTRATIVE INFORMATION

This work was sponsored by the Naval Ship Systems Command under Subproject S4606X, Task 1703.

INTRODUCTION

In the (design of a surface-piercing strut for application to hydrofoil boats, a major problem is to ensure that the side force on the strut will be a predictable, relatively stable, smooth, monotonic function of the local sideslip angle (angle of incidence) at the strut. The importance of this characteristic of hydrofoil struts is illustrated by experience with an early hydrofoil boat which regularly sustained complete loss of lateral stability while running dead ahead, resulting in a spin-out. Suspicion that ventilation of the after hydrofoil struts was the cause of the instability was confirmed when this problem was eliminated after ventilation fences were installed on the struts. Subsequent, investigation into the phenomenon of ventilation has shown that the anomalous changes in side force associated with the inception of ventilation would adequately explain the behavior of that boat.

As applied to a stationary body partially or fully submerged in a flow of water, the term “ventilation” is defined here as the rapid displacement of an extensive region of water or water vapor adjacent to the body by a stable, air-filled cavity attached to the body and connected with the atmosphere. Upon ventilation, side forces on struts have often been observed to increase in magnitude as much as 150 percent of their former value and to reverse their direction of action! These reversals take place after only infinitesimal changes in independent parameters such as speed or sideslip angle. Consequences of this type of behavior on forces acting on a hydrofoil craft hardly need to be elaborated.

Because of the complex and little understood nature of the flow around a surface-piercing strut operating in a partially cavitating regime, theoretical analysis' of the forces on such a strut has been completely inadequate. Even if ventilation effects could be neglected, vapor cavitation is present in nearly all high-speed applications of struts and would be sufficient to cause unpredictable, nonmonotonic behavior of strut side forces with attendant undesirable consequences.

In November 1966, the first of a series of experiments on a family of surface-piercing struts was conducted at this Center to obtain a better understanding of the phenomenon of ventilation and to establish a more rational basis for strut design. This was accomplished by systematically varying parameters which were anticipated to be important. Four members of a family of struts were designed to test the effect of variation of leading edge radius. A fifth member had a 2-ft chord, twice that of the others, and was furnished with a removable endplate. Other parameters that were varied include yaw angle (identical to sideslip angle in a towing tank), depth of submergence, and speed. Conditions for ventilation inception (speed, yaw angle, submergence) were noted. The recorded data included three components each of forces and moments, still photographs, and motion pictures.

OUTLINE OF THE EXPERIMENT

STRUT MODELS

Five struts were tested; four of these were a family designed to test the effect of varying leading edge radius. The fifth had a 2-ft chord, twice the chord length of the others. The first four models were of constant section and had a maximum thickness of 0.12 ft at midchord. The leading edge radii were 0.0, 0.0102, 0.0183, and 0.0327 ft; see Figure 1. For convenience, the 1-ft chord struts are referred to as Models 0 to 3 in order of increasing leading edge radius. The 2-ft chord model is designated Model 4. Model 0 (zero leading edge radius) was an ogive section selected to be one limiting member of the family. Other members were selected by applying the criteria that:

1. The section aft of midchord was to be identical for all members – half ogives.
2. The curvature of the section was to be convex outward.
3. The radius of curvature of the section was to be continuous.

As manufactured, the struts differed from the offsets generated by the above requirements by less than +0.040 in. Surface waviness was within LO.005 in.

Model 4 had the same planform and span as Model 2 but twice the chord length. It was designed to explore the effect of scale on the strut characteristics, particularly ventilation. Since Model 4 did not have twice the span of Model 2, they were not fully geometrically similar. A removable endplate was also fabricated for Model 4 to investigate the effect of differing tip conditions on ventilation and other characteristics. The endplate was parallel

sided and semicircular fore and aft. The parallel sides were each 6 in. from the section centerline whereas the fore and aft edges extended 2 and 3 in., respectively, from the leading and trailing edge of the strut.

TEST CONDITIONS

The struts were towed vertically in the high-speed towing tank of this Center at speeds ranging from 4 to 55 knots. Depths were systematically varied from 1 to 3 ft. While speed was held constant, yaw angle (angle of incidence) was varied continuously during the runs at a rate of 1/3 degfsec from 0 to 10 deg port or starboard for the 1-ft chord models and 0 to 15 deg for Model 4. At higher speeds, several runs at the same velocity were required to cover the full range of angles. No difference in force measurements could be detected between runs with continuous or discrete variation of yaw angle.

Figure 2 shows the range of velocities covered by the test presented as these dimensionless parameters: Froude number *F,* Reynolds number *Re,* and free surface cavitation number σ. There parameters are defined here as:

$$F \equiv U/\sqrt{gc}, \quad Re \equiv \frac{Uc}{\nu}, \quad \text{and} \quad \sigma \equiv \frac{\Delta p}{\frac{1}{2}\rho U^2}$$

In the above definitions,

U is the free-stream velocity,

g is the acceleration due to gravity,

c is the strut model chord length,

ν is the kinematic viscosity of water,

Δp is the difference between ambient atmospheric pressure and the vapor pressure of water, and

ρ is the mass density of water.

INSTRUMENTATION

Three components each of forces and moments were sensed using a dynamometer built by Aerojet General Corporation. Signals from the dynamometer were processed through highly accurate electronic conditioning equipment, recorded on magnetic tape *in* digital form, and automatically converted to engineering parameters on a high-speed computer.

Model 4 was instrumented with a matrix of pressure transducers whose outputs were also digitized and recorded on magnetic tape. (The pressure data will be reduced and published in a later report.)

The tests were monitored by both motion and still pictures. The motion pictures were taken through the water surface on one side of the strut at 500 or 5000 frames/sec. These pictures showed the inception, growth, and sweeping away of vapor cavities on the struts and the subsequent inception and development of ventilation cavities. The still pictures were taken from the port side of the strut through an underwater viewing window in the basin. An electronic flash was used to stop action.

SOURCES OF ERROR

As in any experiment, certain inaccuracies resulted from the limitations of the mechanical and electronic components of the experimental apparatus and from techniques of data reduction and analysis. A discussion of the principal sources of error are listed below in the order of increasing significance.

Signal Processing, Data Reduction

Force and pressure signals were conditioned, amplified, digitized, and recorded by highly accurate electronic equipment and were reduced to physically meaningful units by a high-speed computer. Errors arising from this source were at least an order of magnitude smaller than those from the other sources listed below.

Mechanical Alignment

Standard modelmaking practices were followed in the alignment and manufacture of models, dynamometer, and auxiliary equipment. Runs were made with models yawed first to port and then to starboard. No significant difference could be detected. No distinction could be determined between zero yaw as measured mechanically and as indicated by monitoring of hydrodynamic forces. Mean values of forces measured were probably within 2 or 3 percent of true values in most cases.

Towing Carriage Speed Variation

During a run, towing speeds typically varied less than a few hundredths of a knot for speeds up to 45 knots. At 50 knots, a 1/2- or l-knot variation was not atypical. At 55 knots, as much as a 2-knot variation would occasionally be encountered. In computing force coefficients, the average velocity measured during the run was used.

Play in Yawing Mechanism

The models were driven through their range of yaw angles by a worm and sector gear arrangement which had about 1/5 deg of play. This became significant only when unsteady forces were large enough to activate the play.

Interpretation of Unsteady Force Data

Because of cavitation, the forces and moments on the models were highly unsteady. This introduced a large amount of scatter to the data, mostly because unsophisticated visual averaging techniques were used to obtain mean values. This unsteadiness was by far the most significant source of error; it can best be evaluated by noting the scatter of mean force and moment coefficients as presented in the section on force coefficients.

In general, measurement techniques for mean values were within the limits imposed by largely unavoidable error inherent in the unsteady nature of the phenomena studied. Scatter might have been reduced by better data reduction techniques. The natural frequency of the strut-dynamometer system was around 50 cps. This frequency response appeared to be adequate to obtain the mean change in forces due to ventilation which took place over 0.1 or 0.2 sec. Measurements of periodic cavity shedding indicated that frequencies were present up to 100 cps, for which few components in the experimental system were adequate to measure or record.

RESULTS

VENTILATION

Several different types of ventilation have been observed on partially submerged moving bodies. At low speeds, stagnant water comprising a region of separated flow adjacent to the body is displaced by atmospheric air. At high speeds, the gases comprising a vapor cavity play the same role as does the separated water region at low speeds. A characteristic of all types of ventilation is the displacement of a stagnant or "low energy" fluid region by air. This is accompanied by further changes in the flow, some of which are manifested by an enlargement of the displaced region. Thus a completely new flow regime is established. Furthermore, the previous nonventilated regime usually cannot be reestablished simply by restoration of the previous conditions on the fluid boundaries. This results in a characteristic hysteresis effect.

In addition to the distinction between ventilation at low and at high speeds (with or without vapor cavitation), there is also a distinction between the occurrence of ventilation on bluff bodies and on streamlined bodies yawed with respect to oncoming flow. On a bluff body, ventilation is characterized by a gradual drawdown, with increasing speed, of the water surface in the separated wake region; see Reference 1.* On a yawed, streamlined body, ventilation may occur on the suction side of the body with the sudden displacement by air of a separated region of water associated with stall caused by too great a yaw angle; see Reference 2.

*References are listed on page 38 and followed by a Bibliography of additional studies relevant to this report.

The results of this series of tests show that the type of ventilation which is likely to occur on high-speed hydrofoil craft is intimately connected with vapor cavitation. In a typical test condition, patches of vapor cavitation form on the leading edge of the strut and grow with increasing speed or yaw angle. Figure 3 is an example of the development of this type of cavity. As speed and/or yaw angle continues to increase, the leading edge vapor cavity spreads vertically downward to the tip of the strut and upward nearly to the water surface. Then the cavity extends aft until it fully covers the side of the strut except for a thin sheet of water separating it from the free surface. Eventually, this thin sheet of water is breached, allowing air to "blow out" the vapor cavity, and resulting in a vented cavity which envelops the entire "suction" side of the strut and extends for an undetermined length downstream. Figure 4 is a. photograph which captured the instant of inception. Figure 5 shows the intermediate stage in which air is blowing out the cavity, and Figure 6 depicts fully steady, postvent conditions.

These photographs illustrate some of the radical changes in flow pattern which accompany high-speed ventilation. Unsteady aspects of the flow associated with the periodic shedding of the vapor cavity were immediately eliminated. Spray sheets and rooster tail became nearly vertical and appeared to increase in intensity, although these observations were hindered because of the necessity for shielding equipment from the spray.

The most striking aspect of the ventilation phenomenon was the change in direction and magnitude of the side or "lift" forces. Postvent forces were sometimes half again as great as forces prior to ventilation and oppositely directed. Figure 7 is a time history of side force, drag, and yaw angle during a typical transition from nonventilated to ventilated flow. The whole process from preventilation conditions to fully developed postventilation conditions takes no longer than 1 sec. Most changes take place during the initial 0.1 to 0.2 sec.

Figure 8 shows some of the force oscillations caused by periodic shedding of the vapor cavity (Figure 9), which often preceded ventilation. Although the dynamometer used to monitor forces was not designed to measure unsteady loads, periodic forces are estimated to have ranged from 10 to greater than 35 percent of the mean load.

Effect of Leading Edge Radius on Ventilation Boundary

The maximum speed and yaw angle, and the minimum cavitation number which a given strut, geometry may sustain in an undisturbed environment without the occurrence of ventilation constitute a ventilation boundary.

Figures 10 and 11 show the effect of leading edge radius on ventilation boundaries. In undisturbed flow, resistance to ventilation apparently increases with increasing sharpness of nose shape. This correlates directly with the differences observed in the vapor cavitation characteristics of the several struts. It was stated earlier that, typically, a vapor cavity

would form on the leading edge of the strut models as speed and yaw angle increased. The behavior of the cavity on strut Model 0 (the sharp-nosed ogival section model) was an exception. Under certain conditions, a cavity would first form at midchord on this strut; then, with increasing severity of yaw angle, a second cavity would start at the leading edge and eventually merge with the midchord cavity (Figure 12). The different cavity shape in which this development results can be seen by comparing the two photographs in Figure 13 which show Models 0 and 3 (least and greatest leading edge radius) under similar conditions. Notice that the cavity has not approached as closely to the surface on Model 0, and further, that the shape of the upper boundary of the cavity does not match the shape of the water surface nearly so well as the cavity on Model 3. As these observations suggest, Model 3 is indeed more susceptible to ventilation than Model 0 or any of the sharper nosed struts.

Before concluding that sharp-nosed struts are more resistant in general to ventilation than blunt-nosed struts, it must be pointed out that Model 0 was the only strut which could be observed to "accidentally" or unexpectedly ventilate when acted on by a transient disturbance such as resulted from backing the towing carriage through the wake of the previous run. Even though this phenomenon of unexpected or accidental ventilation was observed only at low speeds (about 5 knots), this experience warns that sharp-nosed struts may possibly be more susceptible to ventilation under at-sea conditions where random disturbances abound.

Effect of Submergence and Endplate on Ventilation Boundary

Figures 14 and 15 show the effect on the ventilation boundaries of size and submergence aspect ratio. Here, submergence aspect ratio is the ratio of submerged span to chord length.

For aspect ratios less than 1, the effect of submergence on cavity development and consequently on ventilation inception was marked. With decreasing aspect ratio, the model became more resistant to cavitation and ventilation. This correlates with the fact that load coefficients and hence pressure variations decrease with aspect ratio. Figures 16 and 17 show cavity development on Model 2 for aspect ratios of 0.5 and 0.875, respectively.

The fact that ventilation boundaries are not significantly affected by increasing submergence beyond an aspect ratio of 1 indicates that the principal factors influencing inception must act very near the surface. That is, tip effects do not become important until they strongly affect the behavior of the flow near the surface.

Figures 14 and 15 also show the effect of the endplate on the ventilation boundaries for Model 4. This was similar to the effect of slightly increasing the aspect ratio. Figure 18 shows cavitation and ventilation on Model 4 with an endplate. Comparing the cavity development with that shown in Figure 16 (no endplate), it can be seen that as close to the surface as 1/4 chord length, shapes of the cavities had already become quite different. With endplate, the tip vortex was eliminated. Despite obvious changes in cavity shape below the surface, the ventilation boundary was only slightly affected. This means that the ventilation

characteristics of struts are determined by the vapor cavity shape very near the surface. Little regard need be paid to the influence of strut-foil-pod intersections, provided the intersection is submerged, say, more than one strut chord length. Again, this conclusion must be tentative, based on the particular mode of ventilation inception encountered during these tests.

Effect of Size on Ventilation Boundary

Comparisons of Model 2 and Model 4, geometrically similar models of different size, revealed no striking differences in vapor cavity development. Figure 19 shows both models under nearly identical conditions of velocity, yaw angle, and submergence aspect ratio. However, a comparison of the force coefficients under the same conditions suggests that the side force coefficients of the smaller model, Model 2, are smaller than those of the larger Model 4. This probably means that despite the apparent similarity shown in the photographs of Figure 19, the vapor cavity was relatively larger on the smaller model, the difference becoming more pronounced for cases in which the cavity extended beyond midchord. The large model was slightly more resistant to ventilation, which would be expected in light of the relatively slower growth of vapor cavitation with increasing speed and yaw angle. Further discussion of this relationship is included in the section on ventilation mechanism.

Effect of Cavitation Number on Ventilation Boundary

Since vapor cavity size and shape appeared to be such an important parameter, it was decided to support a proposal by Lockheed Missiles and Space Company to test Models 0, 2, and 3 in their variable-pressure towing tank where atnbient pressure, and hence cavitation number, can be varied independently of towing speed. The results of this test are reported by Waid.[3]

The ventilation boundaries obtained by Waid are indicated in Figure 20 as cavitation number versus yaw angle. Also shown in the figure are ventilation boundaries obtained at this Center for the same struts at the same submergence. The correlation is only fair. Waid notes that, agreement between the two sets of boundarie s can be improved by computing the cavitation number at a representative depth below the free surface rather than at the free surface as was done in Figure 20. The fact that there is no single representative depth good for all cases indicates that this method of improving agreement is not satisfactory.

In effect, the use of a representative depth as a correction factor is an attempt to account for the fact that, among other things, Froude numbers were not equal in the two facilities. A promising trend is indicated by the boundaries of Model 4 compared to the boundaries of Model 2 obtained under geometrically similar free-surface conditions at this Center and at Lockheed. The cavitation number ventilation boundary for Model 4 was accurately predicted by a I.inear interpolation of Model 2 data obtained at Lockheed for low Froude numbers and at this Center for high Froude numbers.

At the moment, only one case exists for which this Froude number and cavitation number comparison can be made. More data are required before any definite conclusions may be reached. Lockheed plans to test additional geometrically similar models of smaller size, for which the Froude numbers will be closer to the range tested here,, The evidence so far suggests that scaling of Reynolds number may be unimportant compared to Froude and cavitation number scaling, as is true for "ordinary" vapor cavitation phenomena.

Side Force Coefficient as Boundary

The use of the side force coefficient as a ventilation boundary parameter was suggested by Breslin and Skalak.[2] Figure 21 indicates that this scheme collapses the ventilation boundaries for Models 2 and 4 for aspect ratios of 1 or greater. This is reasonable since if cavity (hence flow) similarity in shape and size is the predominate factor influencing ventilation, inception force coefficients should reflect this similarity.

Mechanism of Ventilation Inception

As noted previously in the general description of ventilation, inception occurs when a thin sheet of water separating a vapor cavity from the atmosphere is ruptured. Exactly what factors are responsible for precipitating the final instability of the separating water sheet is a subject of conjecture.

It is known that amplification of small disturbances to the surfaces of a thin sheet of liquid (water) surrounded by a less dense medium (air or water vapor) will occur when the sheet is accelerated in a direction normal to its surfaces. The nature of this instability is the same as that which causes the surface of water in a glass to become disrupted when the glass is suddenly turned upside down. This phenomenon was first treated by G.I. Taylor[4] and is referred to as Taylor instability. Waid[3] suggests that the vorticity cells present in the boundary layer of a strut are amplified by a similar mechanism, finally resulting in rupture. Figures 3d and 4, which are photographs taken just prior to ventilation, certainly suggest that, cavitating vortex cores are indeed connecting the cavity with the atmosphere. However, it is just as easy to convince oneself from the same photographs that the disturbances being amplified, are small surface waves of the type treated by Taylor. Moreover, the amplification of vorticity would seem likely to depend on a viscous mechanism rather than the inviscid Taylor mechanism.

Whatever the initial disturbances, if the assumption is made that they are amplified in the manner suggested by Taylor, some interesting conclusions may be drawn.

The Taylor first-order treatment assumes that the disturbances are small even when amplified. For purposes of this qualitative discussion, it is helpful to assume that when the amplification factor-the ratio of the amplified surface displacement to the original disturbed displacement-reaches a particular value, constant for geometrically similar conditions,

ventilation will occur. If viscosity and surface tension are neglected, the Taylor expression for the amplification factor η/η_0 for disturbances to a thin sheet of liquid whose density is great compared to its surrounding medium is

$$\eta/\eta_0 = \cosh\left(\{-K(g_1 - g)\}^{1/2} t\right)$$

where K is the (dimensional) wave number of the original disturbance,

g_1 is the downward acceleration of the liquid,

g is the acceleration due to gravity, and

t is the elapsed time from the initiation of the acceleration.

The above expression also assumes that the initial disturbances have a wavelength of no more than three times the thickness of the water sheet δ and that they occur in the upper surface only. These last assumptions do not materially affect the conclusions which will be drawn, but they greatly simplify the argument. In the expression for η/η_0, independent variables more appropriate for the strut problem can be used. Let elapsed time t equal ℓ/U, where U is the strut velocity and ℓ the cavity length. Let g_1 equal $\Delta P/\rho\delta$, where AP is the difference between atmospheric and cavity pressure, p is the mass density of the liquid, and δ is the thickness of the undisturbed liquid sheet. The result is

$$\eta/\eta_0 = \cosh\left\{-K\ell\left(\frac{\Delta P\ell}{\rho U^2\delta} - \frac{g\ell}{U^2}\right)\right\}^{1/2}$$

Thus it can be seen that the stability of the thin sheet of water separating the cavity from the atmosphere is a function of $\Delta P/\rho U^2 = \sigma$, the free surface cavitation number; $g\ell/U^2 \equiv 1/F_\ell^2$, the reciprocal of the square of the Froude number based on cavity length; ℓ/δ, the ratio of the cavity length to water sheet thickness; and $K\ell$, the ratio of the cavity length to the length of the initial disturbance. Cavity similarity can be approximately achieved if the cavitation number and chord length Froude number are scaled. Therefore, the Froude number based on cavity length may be replaced by a Froude number based on chord length times a factor which is a function of chord length Froude number and cavitation number.

Emmons et al.[5] treat second and third order effects, surface tension, and viscosity. The effect of viscosity is small and serves only to provide some damping to the amplification factor. Surface tension also is unimportant except that it results in a "cutoff" wave number for disturbances above which the first-order treatment shows no amplification.

The foregoing; discussion indicates that modeling of ventilation inception due to vapor cavitation will entail scaling of surface cavitation number and Froude number based on any model dimension, as well as some assessment of the effect of various types of disturbances. The effects of surface tension and viscosity are relatively unimportant. Furthermore, the

large factor ℓ/δ which appears in front of the cavitation number in the expression for amplification factor indicates that σ is much more important than F. Experience and available experimental evidence tend to support these conclusions although more data are necessary. Postulating Taylor instabilities as the mechanism for final rupture of the water sheet reduces the problem of determining inception conditions to the more familiar problem of predicting vapor cavity dimensions. The Taylor mechanism-or for that matter, any mechanism which does not depend on viscosity or surface tension-will similarly "reduce" the problem to one depending primarily on Froude and cavitation numbers. Again, these remarks apply only to the mode of inception considered here.

FORCE COEFFICIENTS, HYSTERESIS

The mean side and drag forces on the struts were reduced to dimensionless coefficients by dividing by $1/2\rho U^2$ A, the dynamic pressure times A, the nominally submerged area. Mean values were obtained by fairing a straight line through the unsteady data. Figures 22 through 34 are graphs of the mean force coefficients showing the effects of the various test parameters. One of the most interesting and significant features of ventilated flow is the reversal of "lift" or side forces. The magnitude of the reversed side force was often gteater than the side force measured prior to ventilation. Actually, this reversal is a consequence of the general hysteresis effect which ventilated flow regimes exhibit. At yaw angles below which spontaneous ventilation will occur, the existence of a stable, ventilated flow regime is still possible. Force coefficients were obtained for these regimes either by artifically inducing ventilation by disturbing the water ahead of the strut or by reducing the angle of attack after natural inception of ventilation. Figures 22 and 23 illustrate the lift and drag hysteresis loop for Model 4. Note that vented forces are somewhat insensitive to yaw angle.

Ventilation was found to persist and to continue to exhibit force characteristics significantly different from nonvented regimes even when the yaw angle was reduced to zero. Persistence could be observed and evidence of persistence can be seen in Figures 22 and 23, even when the yaw angle was decreased to -0.5 deg. That is, the vented flow persisted as yaw angle decreased through 0 deg and somewhat beyond. As can be seen from Figures 22 and 23, the ventilated regimes were rather unstable below some yaw angle.

The chordwise variation in position of the center of pressure aft of the leading edge is indicated at appropriate points on the curve of Figure 22. These were computed from moment data collected. As the vapor cavity developed, the center of pressure shifted from the quarter chord position at small angles to midchord as ventilation inception angle was approached. After ventilation, the center of pressure shifted to 0.8 chord. Since the ventilated side forces were directed oppositely from the forces before ventilation, the yaw moment about the centroidal axis retained the same sense as before ventilation.

Figures 24 and 25 are photographs of a sequence of runs in which angle of yaw was increased to the vent boundary, and then reduced. Note that with decreasing yaw angle, the vented cavity may not extend to the full depth of the strut and that there may be several separate points of attachment. A comparison of the first photograph in Figure 24 and the last two in Figure 25 illustrates the persistence of the vented cavity.

The significance of these observations is that a ventilated regime is possible at any yaw angle, including zero. Presumably all that would be required to initiate such a regime would be a sufficient disturbance. The undesirability of this behavior for ship applications is obvious.

Nonl inearity

A glance at the plots of force coefficients versus angle of yaw shows that at speeds greater than 30 knots (51 fps), the response of the forces to changes in angle of yaw was highly nonlinear, becoming more so with increasing speed. Two principal nonlinear regimes may be noted. In the first, side force (lift) coefficient slopes increased steeply with increasing speed at low yaw angles. This was associated with the growth of a leading edge cavity. The second regime was characterized by a falling off of side forces with increasing yaw angle-a "flat response" region-associated with large angles, large vapor cavities, and high speeds. The higher the speed, the smaller the angle of yaw at which the flat response regime began. At 55 knots, the side force response of Model 1 became practically flat beyond an angle of yaw greater than 1 1/2 deg. Low aspect ratios inhibit cavitation and consequently nonlinear behavior.

The implication of the flat response region is that even without ventilation, ordinary cavitation would be sufficient to precipitate a potentially unstable situation at much lower angles of incidence than those for which spontaneous ventilation inception has been observed.

Effect of Leading Edge Radius on Force Coefficients

Figures 26 through 30 show the effect of leading edge radius on force coefficients. The general trend is that the smaller the leading edge radius, the greater the linearity and the less severe the reversals of side force on ventilation. This reflects in part the reduced tendency towards cavitation of the finer nosed struts.

Effect of Size on Farce Coefficients

There were no striking differences in the behavior of Models 2 and 4 although, as mentioned, for similar aspect ratios and speeds, the ratio of cavity length to chord length appeared somewhat larger on the 1-ft chord model (Model 2) than on the 2-ft chord model (Model 4). This conjecture is supported by Figure 31 which compares the side force coefficients of Models 2 and 4 at an aspect ratio of 1. For speeds above 45 knots (76 fps),

the coefficients were distinctly lower for the smaller model on the "flat response" part of the curves, suggesting that the cavity sizes *are* relatively larger on the smaller model. This being the case, then, consistent with the earlier discussion of mechanism, the larger model should be (and is) more ventilation resistant than the smaller model.

Effect of Submergence and Endplate on Force Coefficients

Figures 32, 33, and 34 show the effects of aspect ratio and endplate on the side and drag force coefficient curves of Model 4. Figure 26 also includes several theoretical curves.[6, 7] For aspect ratios less than I, the difference in value of side force coefficients after ventilation was approximately a constant with respect to aspect ratio. However, because increased aspect ratio decreases the angle of attack vent boundary, the coefficient reversals tended to become proportionately more severe with increased aspect ratio or addition of an endplate. Over the limited range examined, beyond an aspect ratio of 1 ventilated force coefficients became more or less independent of aspect ratio, angle of attack, and speed. As previously mentioned, the side force coefficient curve near the ventilation boundary (flat response regime) becomes flatter as the aspect ratio increases until an aspect ratio of one is reached:, see Figure 33. The corresponding curves for drag coefficient are shown in Figure 34. The highest aspect ratio tested with Model 4 was 1.5. Figure 33 presents the side force coefficient **versus** yaw angle at this aspect ratio for a range of speeds from 10 to 55 knots (17 to 93 fps).

SUMMARY OF CONCLUSIONS

VENTILATION BOUNDARIES

1. *Relation to vapor* cavitation: At high speeds, ventilation inception is intimately connected with the **shape** and extent of the associated vapor cavity, and it is the rupture of this cavity which results in ventilation.

2. *Effect of strut* leading edge radius: For initially undisturbed conditions, struts with sharp leading edges are more resistant to ventilation at high speeds than are blunter struts. This correlates with the effect of leading edge radius on vapor cavity shape.

3. *Effect of* size: Increase of size is accompanied by a decrease in relative cavity size, and hence a decrease in susceptibility to ventilation.

4. *Effect of submergence and endplate:* Ventilation susceptibility increases with aspect ratio up to somewhat beyond aspect ratio 1. Beyond that, it is relatively insensitive to aspect ratio. An endplate has the same effect on ventilation as an increase in submerged length equal to the half-width of the endplate.

SCALING VENTILATION

Experience, experimental evidence and some analysis indicate that the mechanism of ventilation is relatively independent of the effects of viscosity and surface tension. Therefore, modeling should be possible in the same way that vapor cavitation is modeled, i.e., Froude and cavitation number scaling.

FORCE COEFFICIENTS

1. *Hysteresis:* A pronounced hysteresis phenomenon is associated with ventilation; one of the results of this is a possible severe change in the magnitude and direction of side forces, with obvious dangerous implications for hydrofoil craft.

2. *Unsteadiness:* Ventilation is usually preceded by unsteady, nonlinear forces associated with cavitation. Upon ventilation, the unsteadiness disappears.

3. Nonlinearity: Aside from ventilation, the,effects of cavitation result in extremely nonlinear behavior of side force versus yaw angle. This could easily result, in unstable situations for a hydrofoil craft.

4. *Effect of leading edge radius:* Finer nosed struts respond more linearly and are less susceptible to severe reversals upon ventilation than more blunt struts.

5. *Effect of size:* Because of relatively smaller vapor cavities, larger struts tend to preserve greater linearity of response to changes in yaw angle.

6. *Effect of aspect ratio and endplate*: In the absence of cavitation, theory adequately predicts the effect of aspect ratio over the range of Froude numbers tested. In the cavitating and ventilating range, increasing aspect ratio increases coefficients, decreases linearity, and tends to make force reversals on ventilation more severe. Beyond an aspect ratio of 1, these tendencies become less pronounced. An endplate has about the same effect on force coefficients as an increase in submerged length equal to the half-width of the endplate.

RECOMMENDATIONS

1. There is some indication that the presence of disturbances such as waves or damaged strut contours may radically alter the conclusion that sharp-nosed struts are more resistant to ventilation than are blunt struts. This must be investigated before a study of optimum shapes can be rationally pursued.

2. The only way in which a valid comparison can be achieved between models tested at Lockheed Underwater Missile Facility and full-scale struts is to utilize observations on a full-scale craft. A comparison based on preservation of Froude and cavitation numbers cannot readily be made between models tested at Lockheed and geometrically similar models at this Center. For a given size of model which could be conveniently tested at Lockheed, the

corresponding size, which preserved both Froude and cavitation number at NSRDC, would be prohibitively large. This is because the only way of achieving low cavitation numbers in the NSRDC towing tank is to use high velocities. This being the case, the only way to reduce Froude numbers to realistic values is to increase the model size beyond a practical point. Conversely, a practical model size for NSRDC testing would entail the use of an unrealistically small model at Lockheed to achieve Froude and cavitation scaling,. Testing of additional sizes of models at Lockheed would extend the range of important parameters closer to those obtainable at this Center. But full-scale observations are desirable for many other reasons, not the least of which is to determine how closely laboratory conditions actually simulate those encountered in operation.

3. More adequate flow visualization techniques should be attempted to further define the mechanism of ventilation inception. Motion pictures taken from below the water surface would be helpful, especially since they would not be obscured by spray as were those taken through the surface.

4. Optimum shapes might profitably be investigated either following the completion of, or simultaneously. with, the preceding suggestions. The shapes investigated should include base-vented and reverse-cusped struts. Experimental investigation should be supplemented by analytical determination of pressure distributions at angles of yaw. (Flat distributions would be preferable.)

5. The effects of sweep and dihedral could be investigated as an adjunct to a study of shapes.

6. Testing at Lockheed should be expanded to include additional sizes of models and the range of test conditions should be extended. This will enable a better comparison with NSRDC results, and consequently improve our understanding of scale effects.

ACKNOWLEDGMENTS

The authors acknowledge the efforts of John Bedel, Peter K. Besch, Michael F. Jeffers, John H. Pattison, and Edwin P. Rood who cooperated in writing programs to reduce the raw data and generate the strut offsets. Mr. Besch also calculated the points in Figure 32 which represent the MIT theory. Thanks are also extended to William G. Souders who contributed to the conduct of the experiment and to H. D. Harper and L. Bruce Moore who provided valuable assistance in the instrumentation and mechanical aspects of the test.

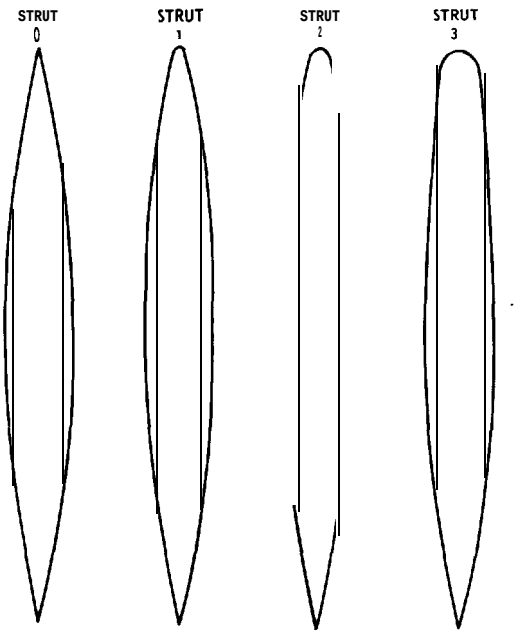

Figure 1 – Family of Strut Shapes

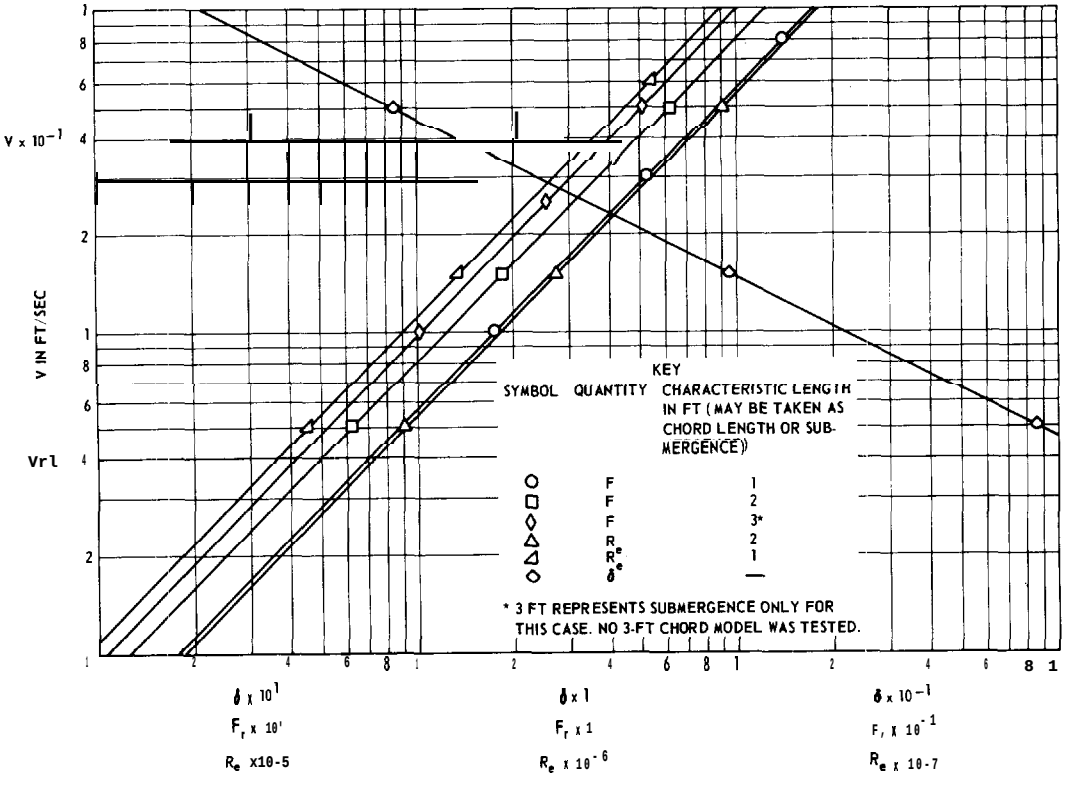

Figure 2 – Froude Number, Reynolds Number, and Cavitation Number versus Velocity for the Range of Conditions Tested

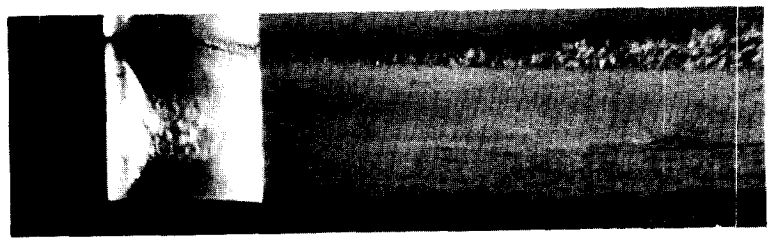

40 Knots, 3.3-Degree Yaw

40 Knots, 10-Degree Yaw

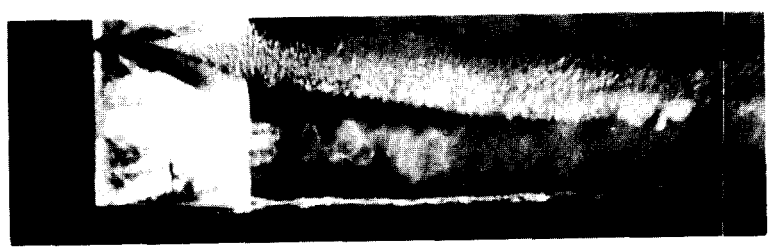

45 Knots, 7.5-Degree Yaw

45 Knots, 10-Degree Yaw

Figure 3 – Typical Development of Vapor Cavity with Increasing Speed and Yaw Angle, Model 2

Aspect ratio 1.

Figure 4 — Inception of Ventilation, Model 1
Yaw angle 10 deg, 45 knots, aspect ratio 3.0.

Figure 5 — Intermediate Postinception Stage, Model 1
Yaw angle 8 deg, 55 knots, aspect ratio 3.0.

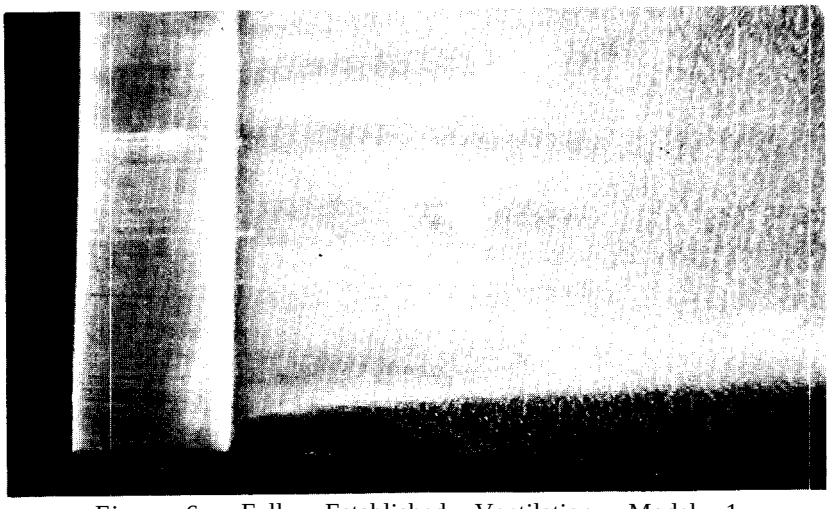

Figure 6 — Fully Established Ventilation, Model 1
Yaw angle 8.5 deg, 50 knots, aspect ratio 3.0.

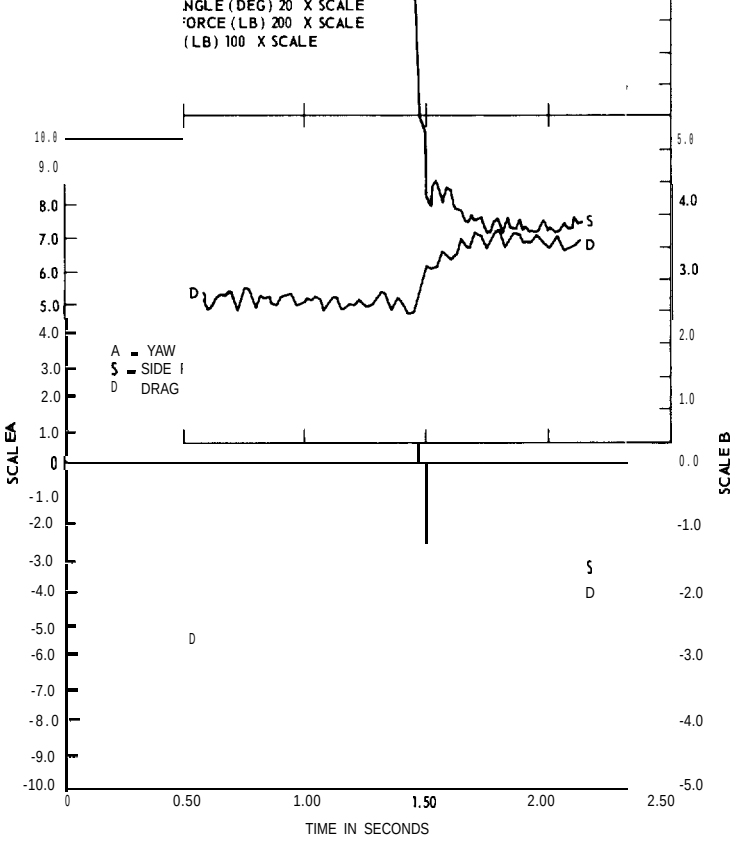

Figure 7 – Side Force, Drag, and Yaw Angle versus Time for a Typical Strut Ventilation, Model 4

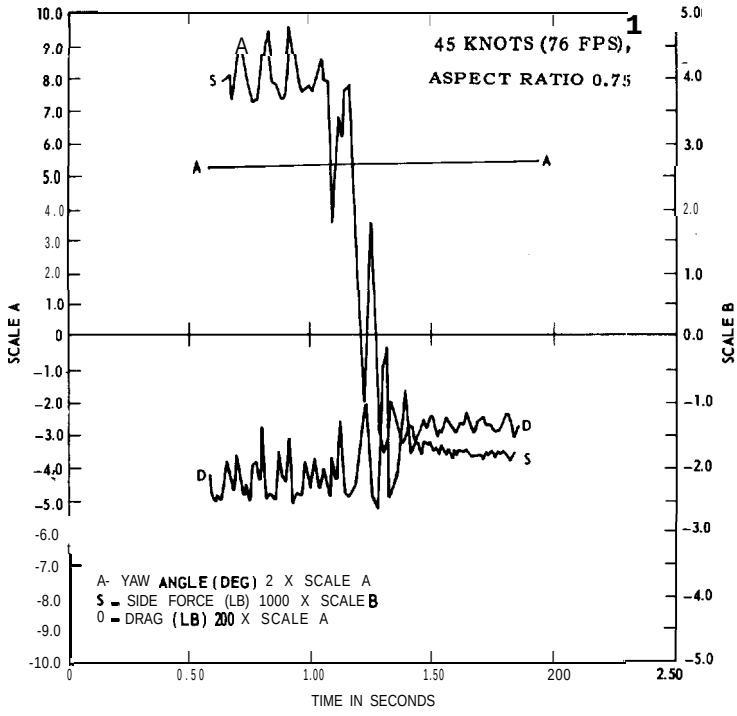

Figure 8 – Side Force, Drag, and Yaw Angle versus Time Showing Preventilation Force Oscillation for Model 4

Figure 9 – Vapor Cavity Being Shed, Model 2

Yaw angle 9 deg, 40 knots, aspect ratio 2.0.

ASPECT RATIO 2

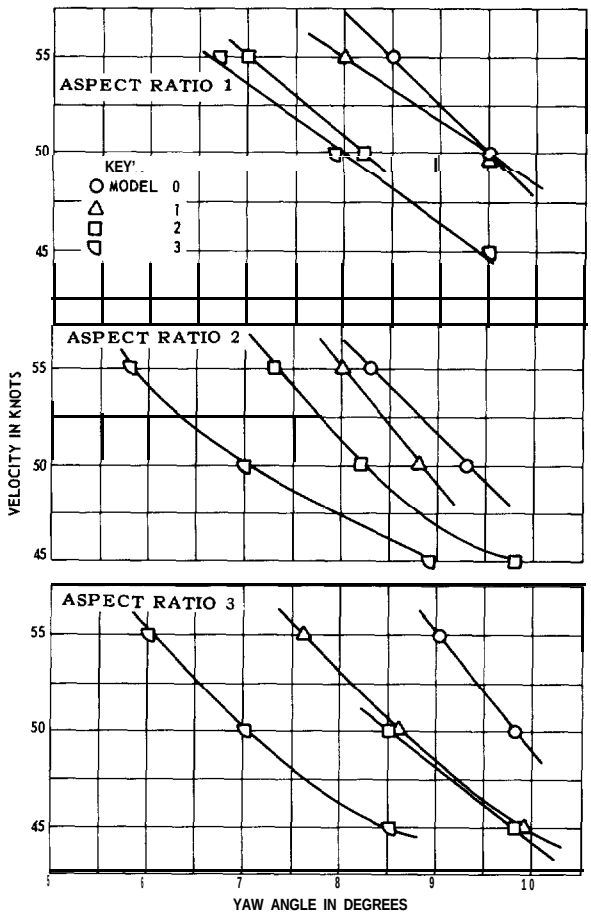

Figure 10 – Velocity versus Yaw Angle on the Ventilation Boundary for Models 0 to 3

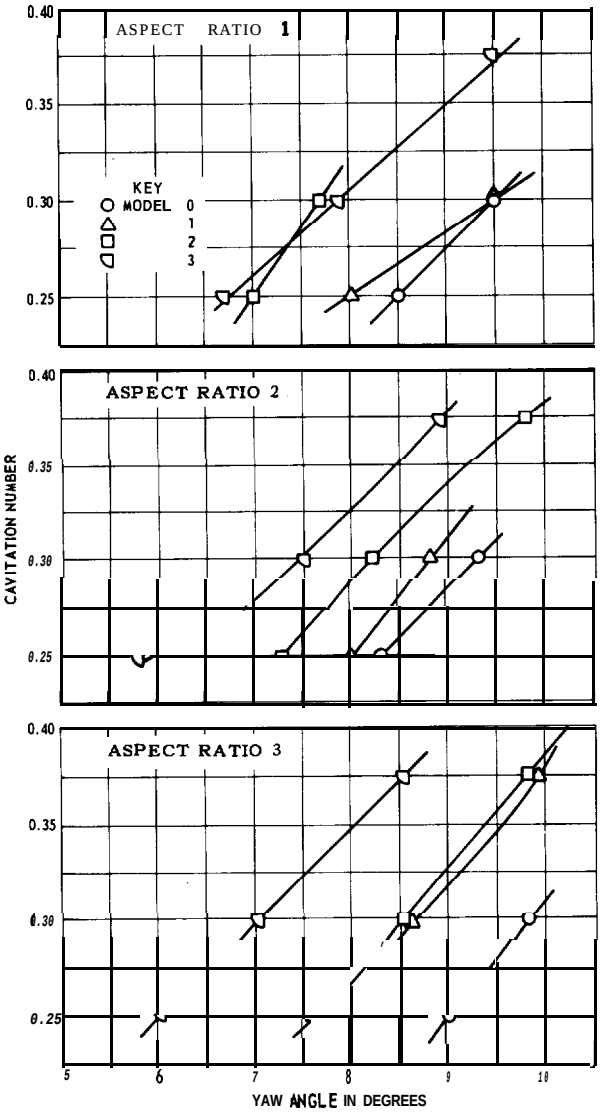

Figure 11 – Cavitation Number versus Yaw Angle on the Ventilation Boundary for Models 0 to 3

Yaw Angle 1 Degree

Yaw Angle 5.5 Degrees

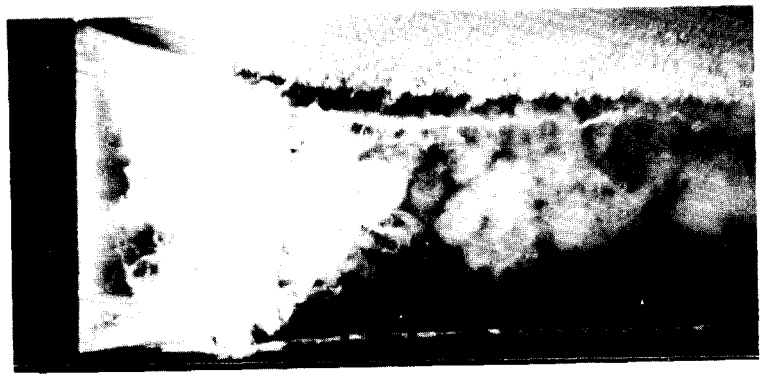

Yaw Angle 8 Degrees

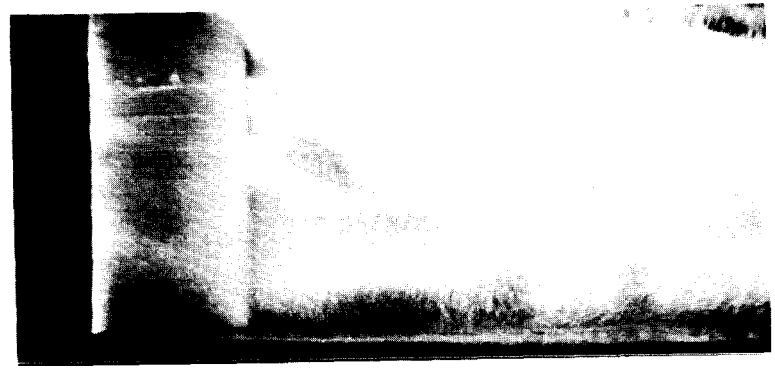

Yaw Angle 8.5 Degrees

Figure 12 – Vapor Cavity Development Typical of Model 0

55 knots, aspect ratio 2.0.

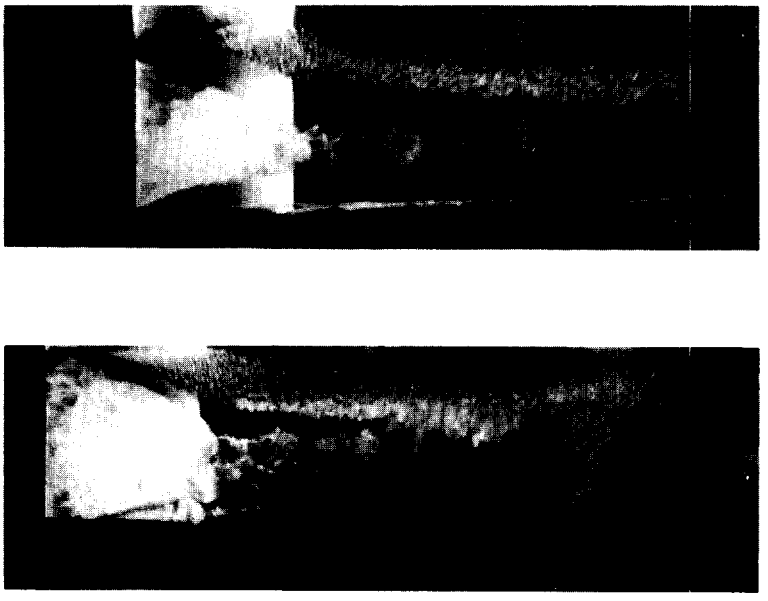

Figure 13 — Differences in Cavity Development for Models 0 and 3 under Similar Conditions

Yaw angle 7 deg, 50 knots, aspect ratio 1.0.

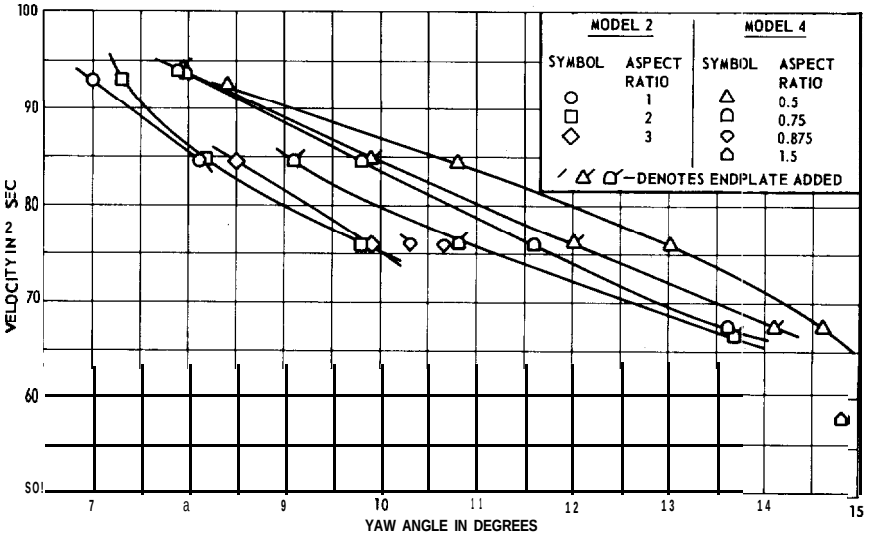

Figure 14 — Velocity versus Yaw Angle on the Ventilation Boundary for Models 2 and 4

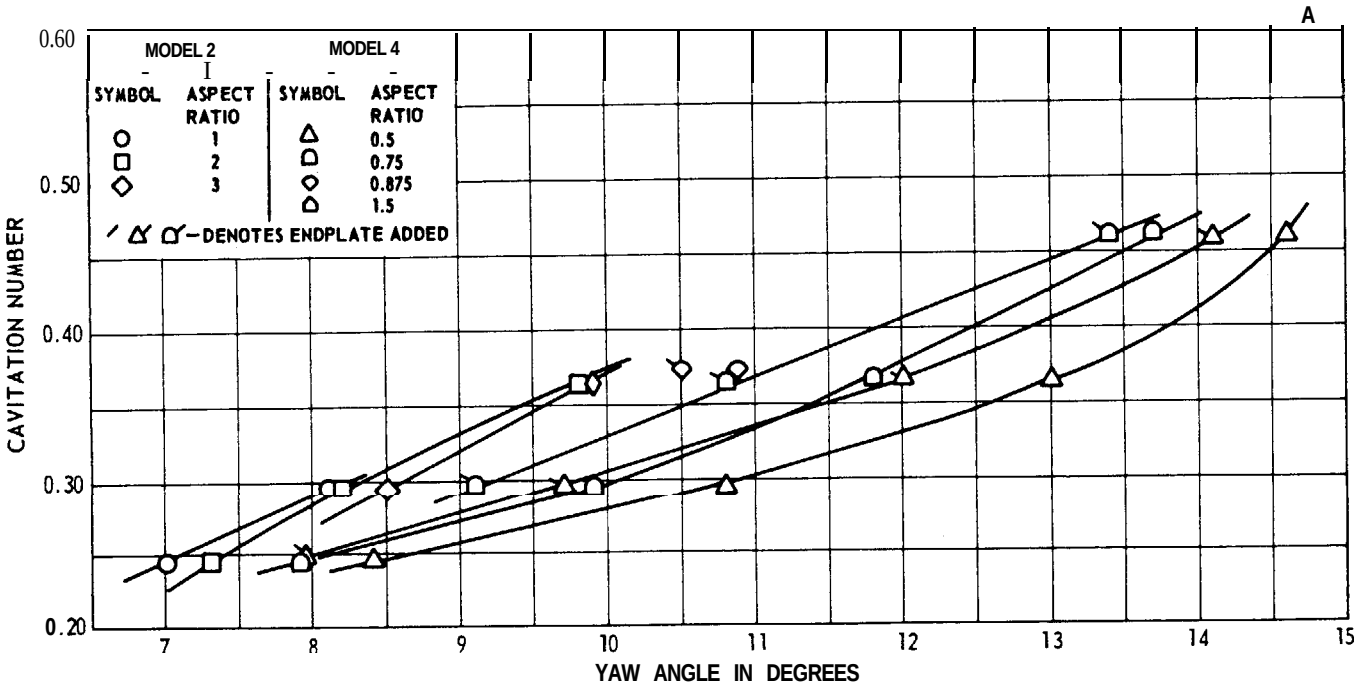

Figure 15 – Cavitation Number versus Yaw Angle on the Ventilation Boundary for Models 2 and 4

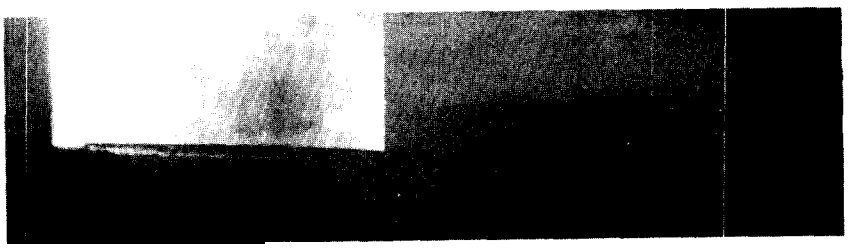

Yaw Angle 3 Degrees

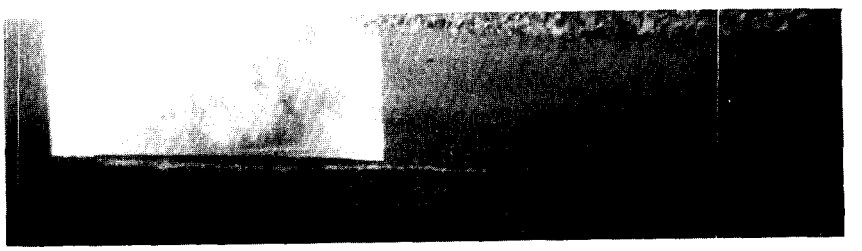

Yaw Angle 7 Degrees

Yaw Angle 11 Degrees

Yaw Angle 12 Degrees

Yaw Angle 13 Degrees

Figure 16 – Cavity Development on Model 4, Aspect Ratio 0.5

At 45 knots.

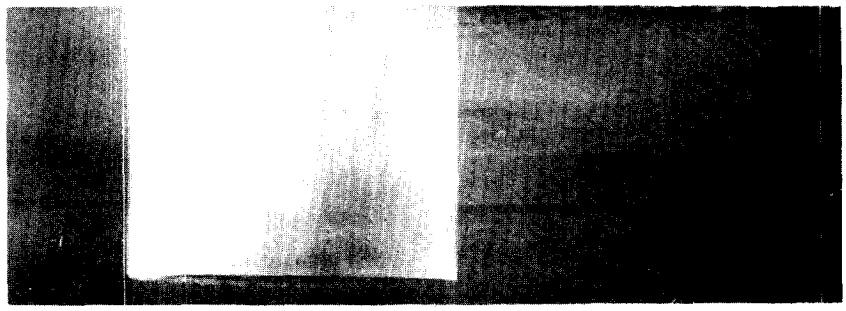

Yaw Angle 3 Degrees

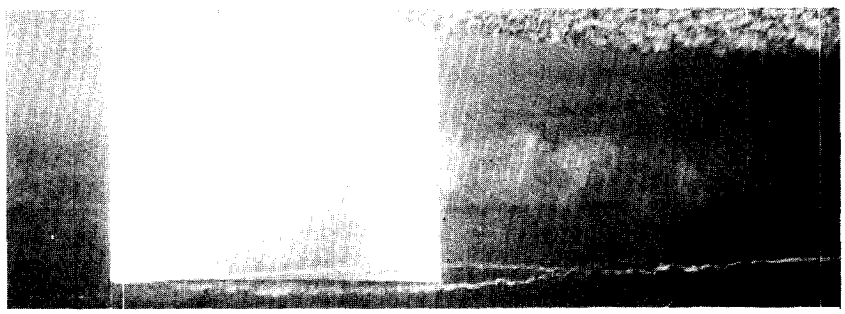

Yaw Angle 5 Degrees

Figure 17 – Cavity Development on Model 4, Aspect Ratio 0.875

At 45 knots.

Yaw Angle 9 Degrees

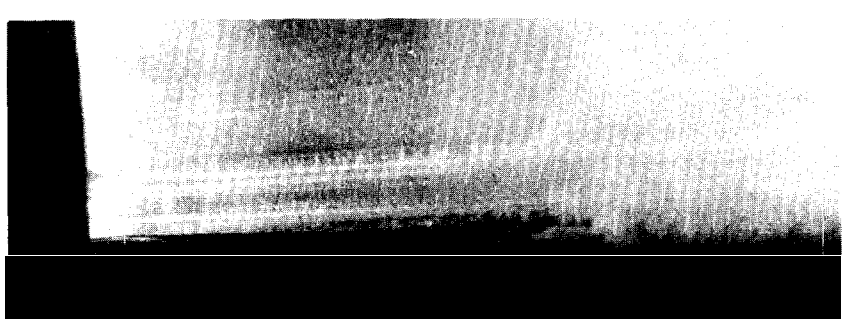

Yaw Angle 10 Degrees

Figure 18 – Model 4 with Endplate

50 knots, aspect ratio 0.75.

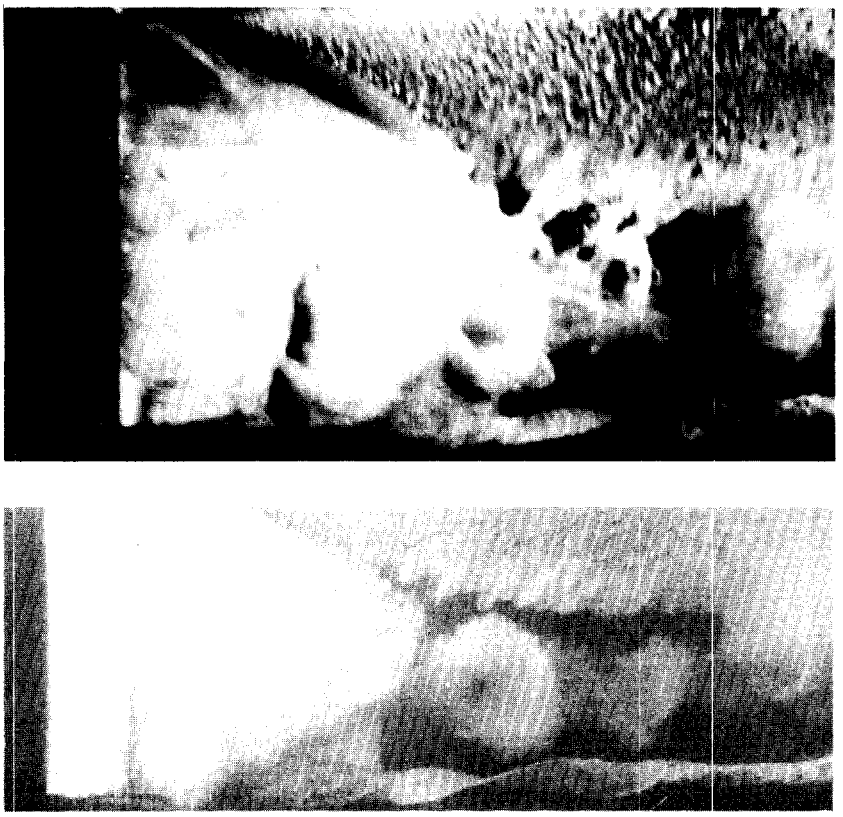

Figure 19 -- 1.0- and 2.0-Foot Chord Models (Models 2 and 4) under Similar Conditions

Yaw angle 10 deg, 45 knots, aspect ratio 1.0.

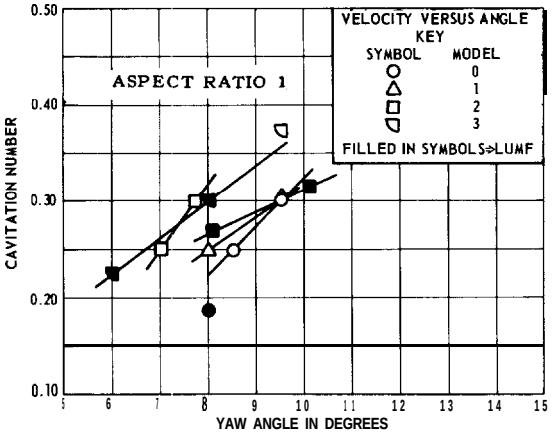

Figure 20 - Cavitation Number versus Yaw Angle on the Ventilation Boundary for Models 0, 2, and 3

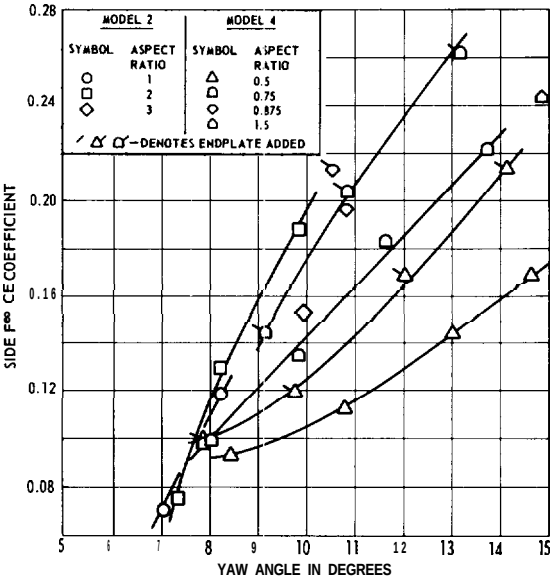

Figure 21 - Side Force Coefficient versus Yaw Angle on the Ventilation Boundary for Models 2 and 4

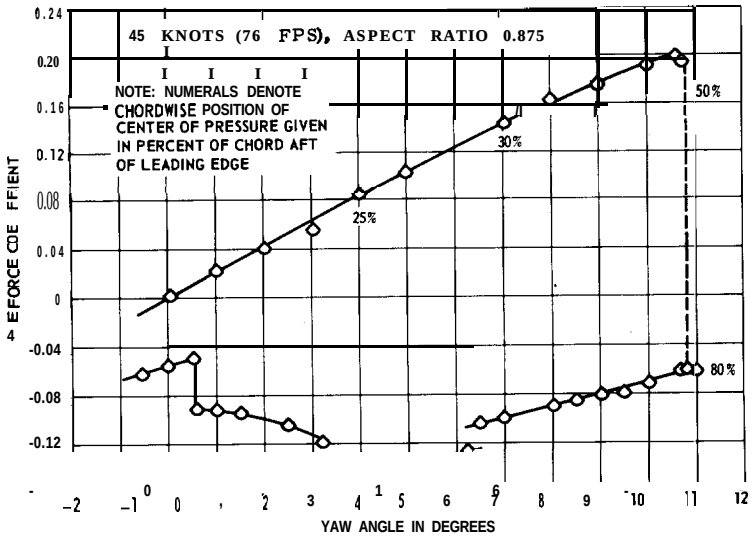

Figure 22 — Hysteresis Loop of Side Force Coefficient versus Yaw Angle for Model 4

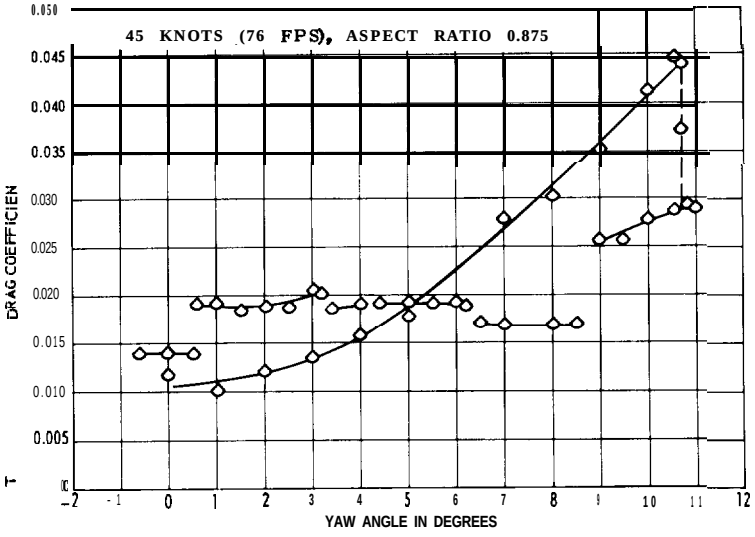

Figure 23 — Hysteresis Loop of Drag Coefficient versus Yaw Angle for Model 4

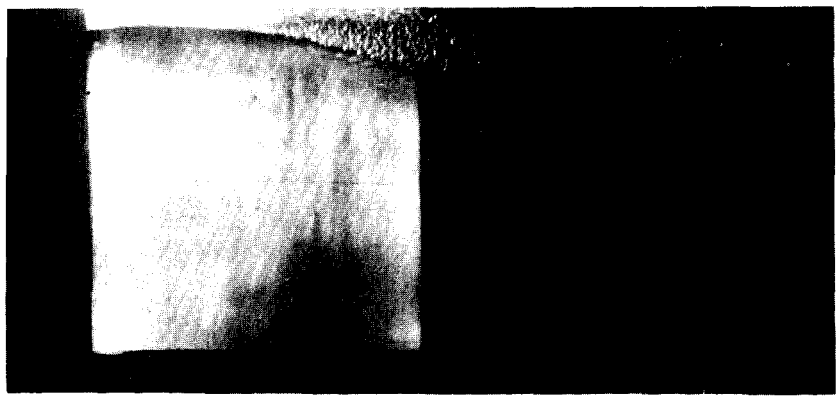

Yaw Angle 3 Degrees

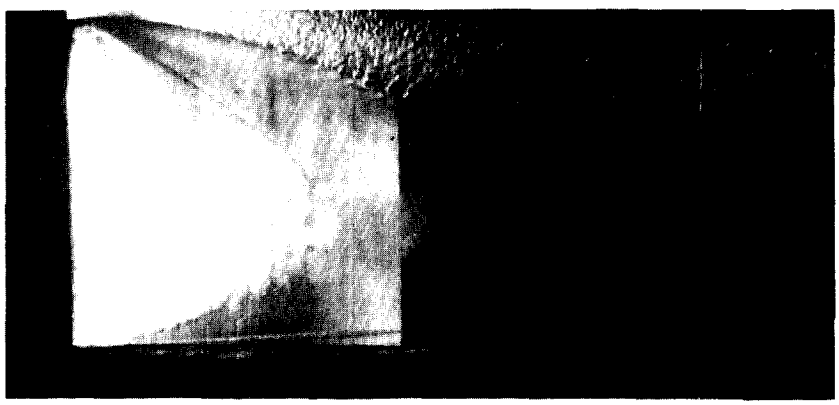

Yaw Angle 5 Degrees

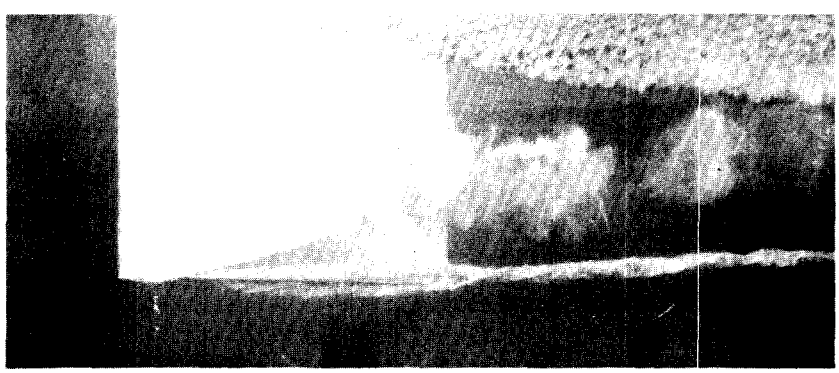

Yaw Angle 8 Degrees

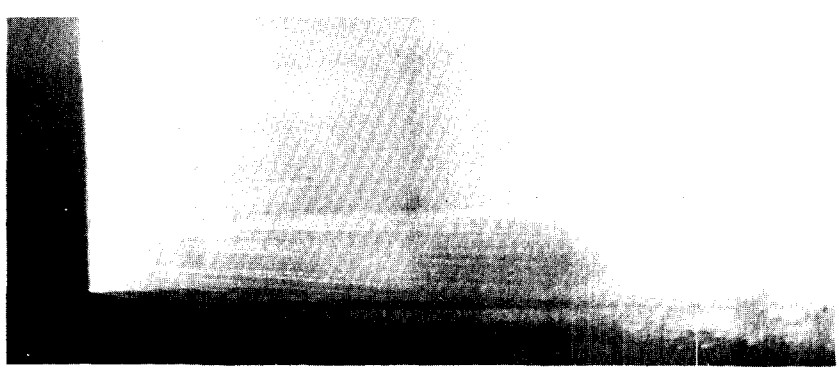

Yaw Angle 11 Degrees

Figure 24 – Model 4, 45 Knots, Aspect Ratio 0.875

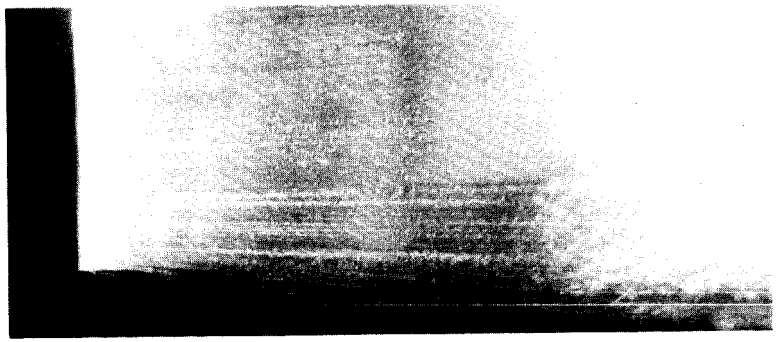

Yaw Angle 9 Degrees

Yaw Angle 7 Degrees

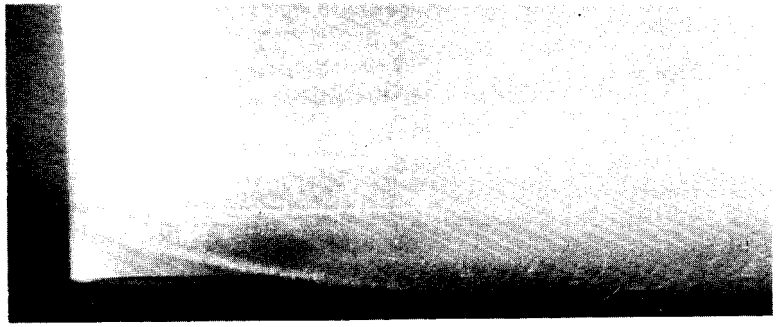

Yaw Angle 4 Degrees

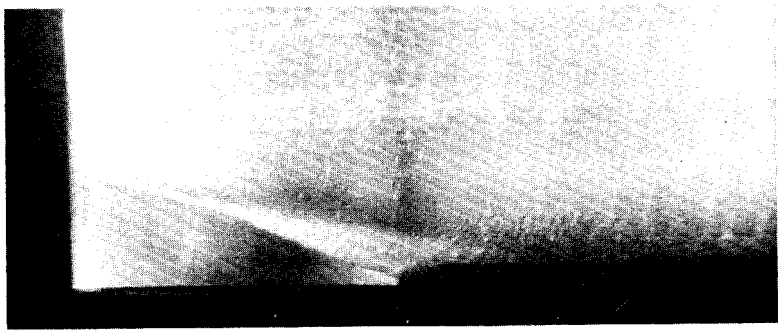

Yaw Angle Less Then 4 Degrees

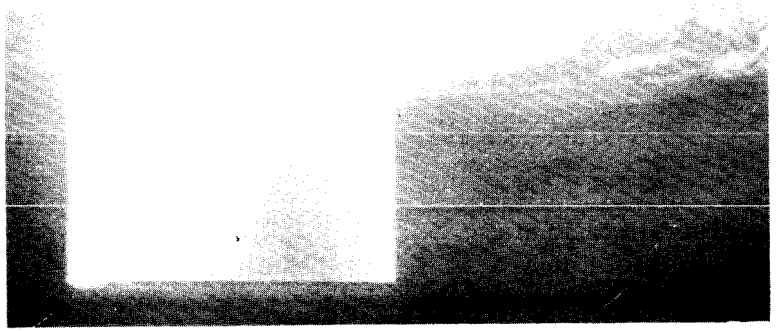

Yaw Angle 2 Degrees

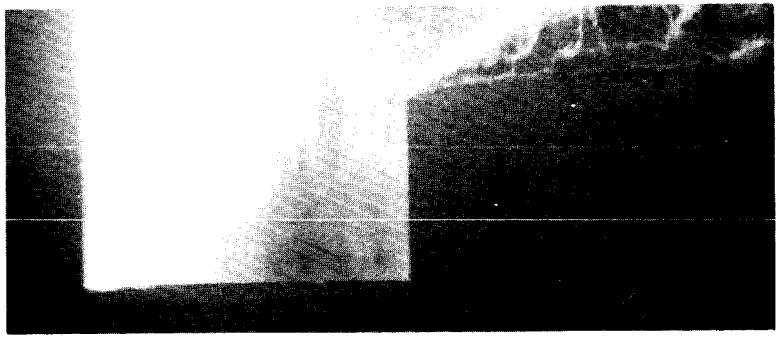

Yaw Angle 0.5 Degree

Figure 25 – Model 4, 45 Knots, Aspect Ratio 0.875

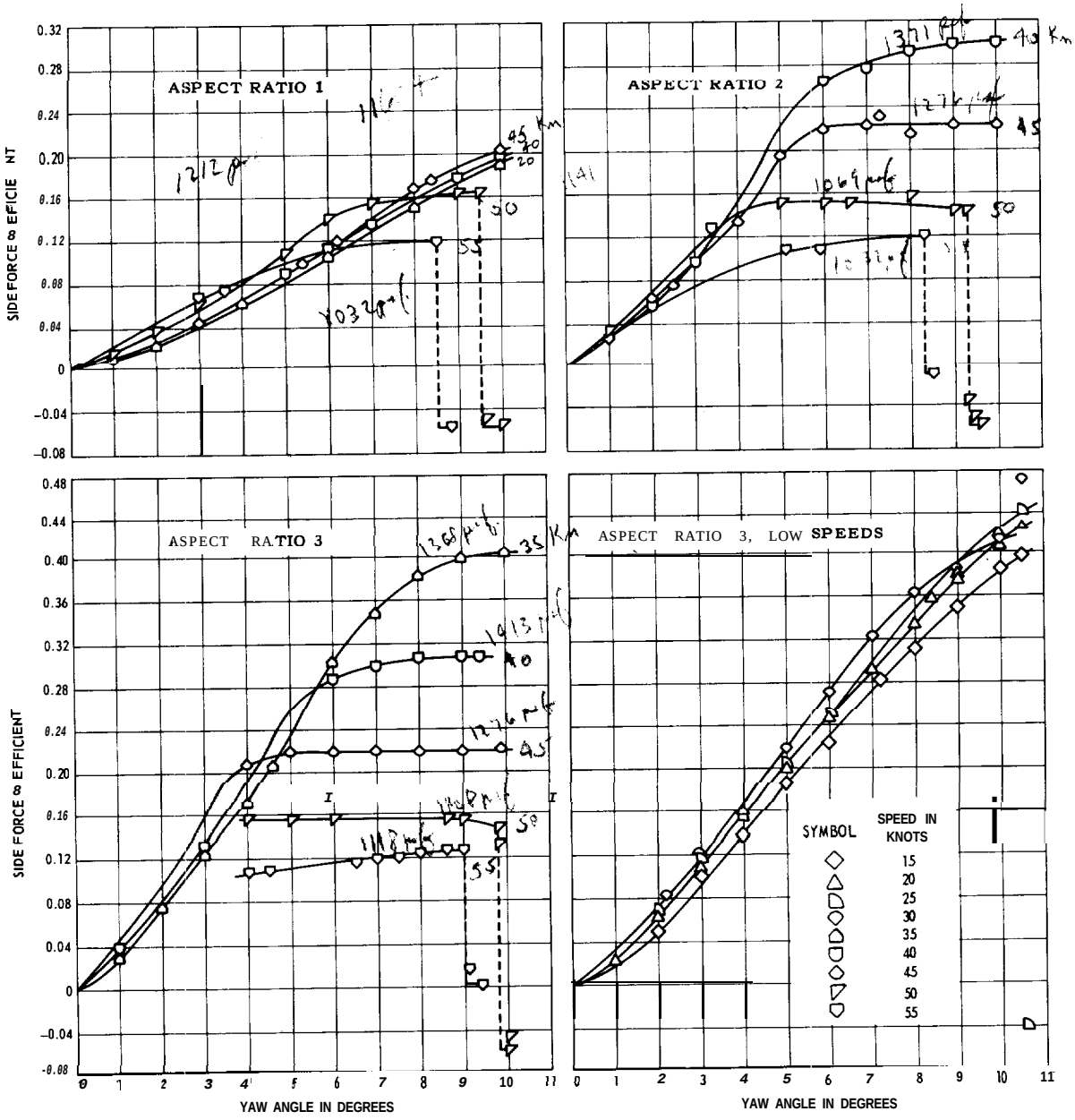

Figure 26 – Side Force Coefficient versus Yaw Angle for Model 0

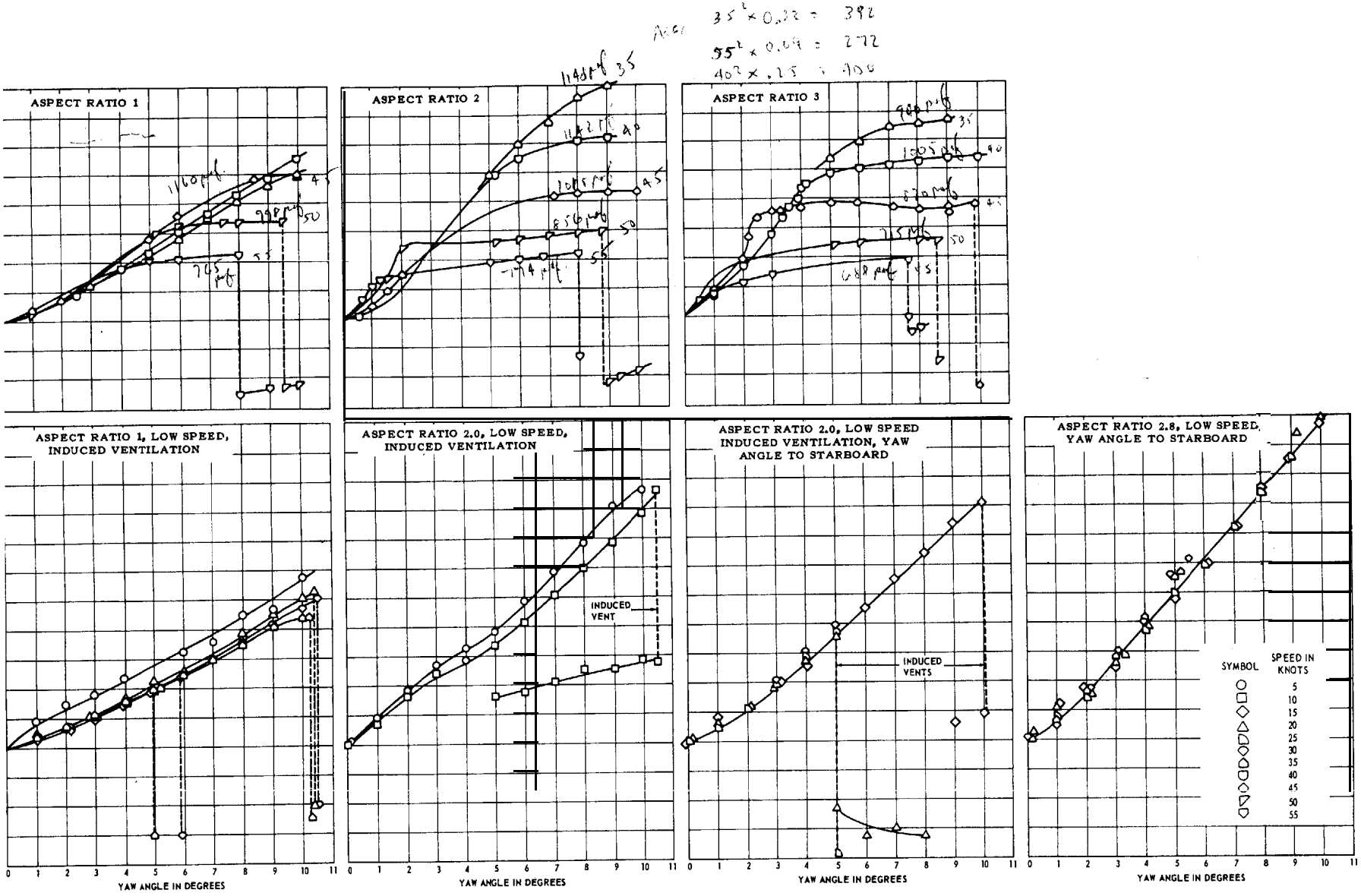

Figure 27 – Side Force Coefficient versus Yaw Angle for Model 1

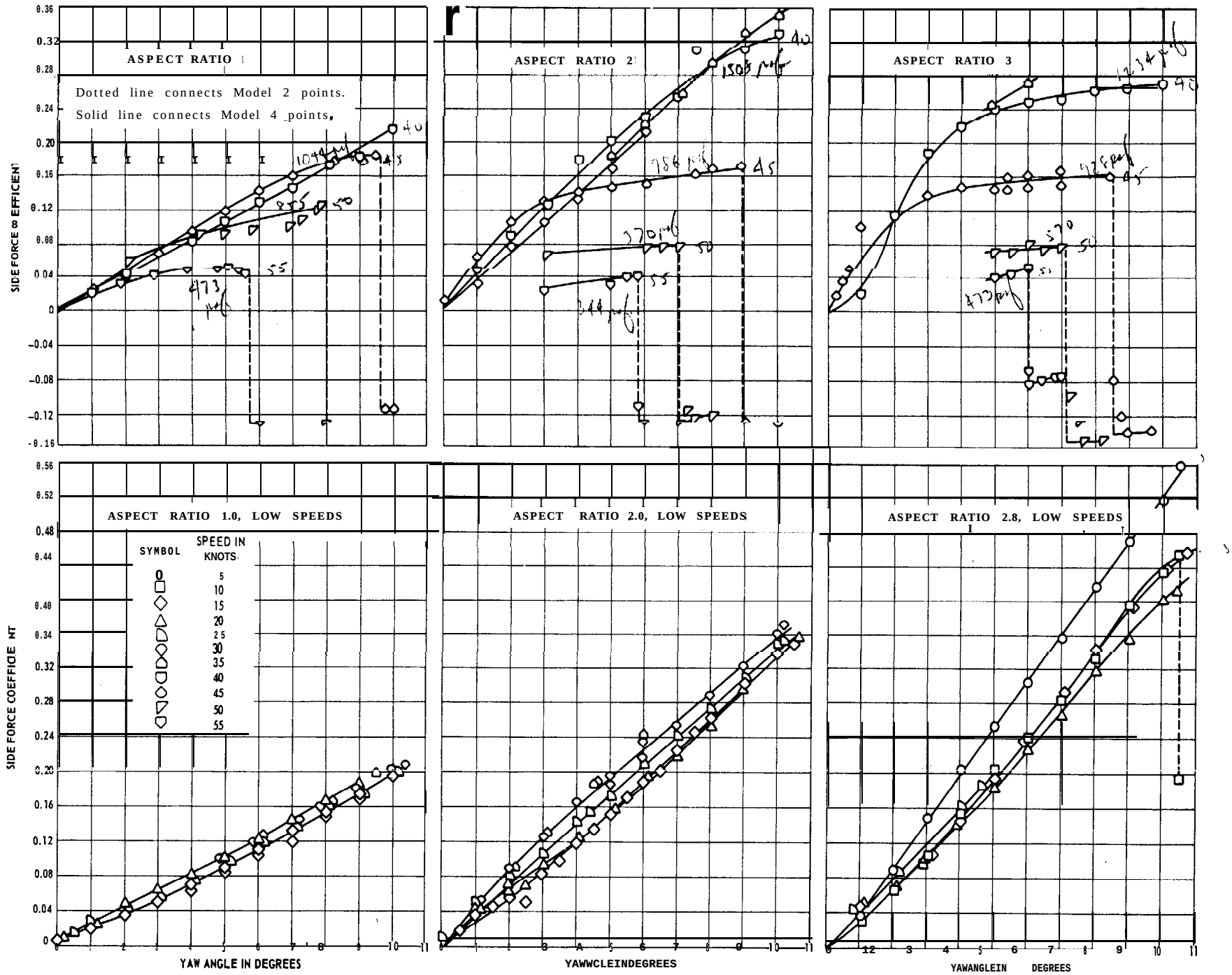

Figure 29 – Side Force Coefficient versus Yaw Angle for Model 3

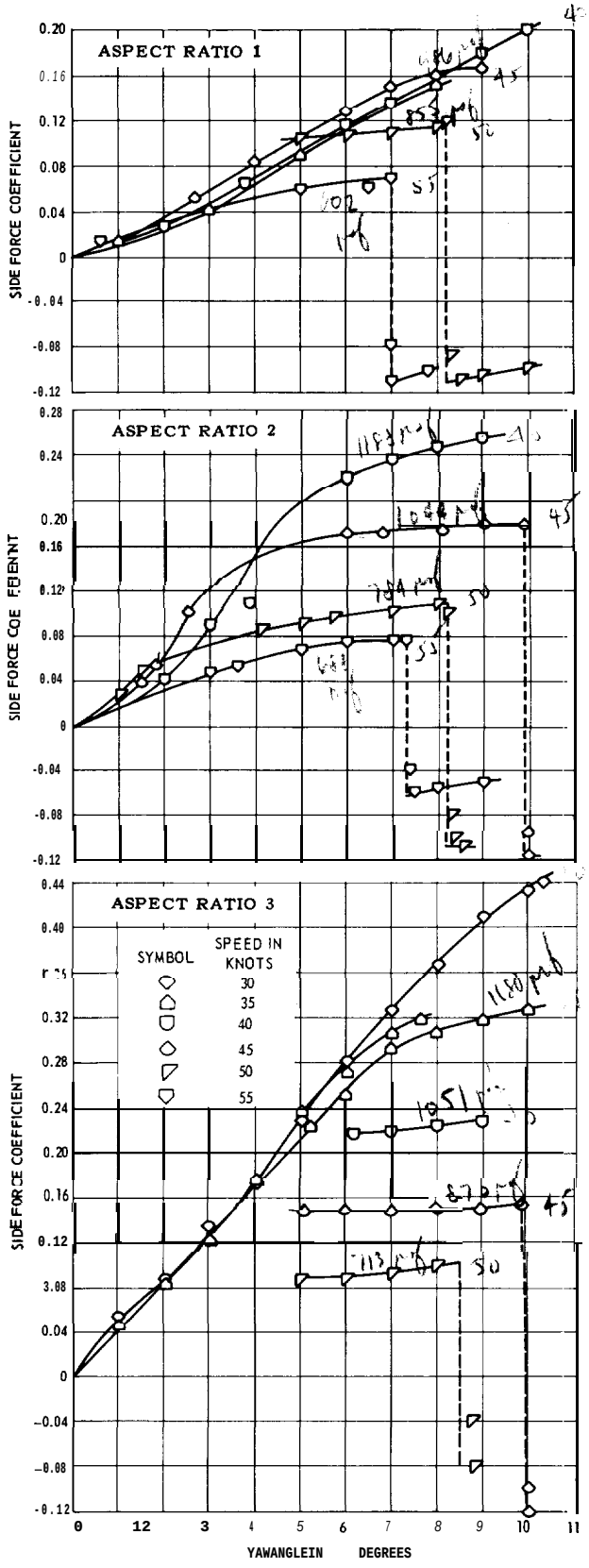

Figure 28 — Side Force Coefficient versus Yaw Angle for Model 2

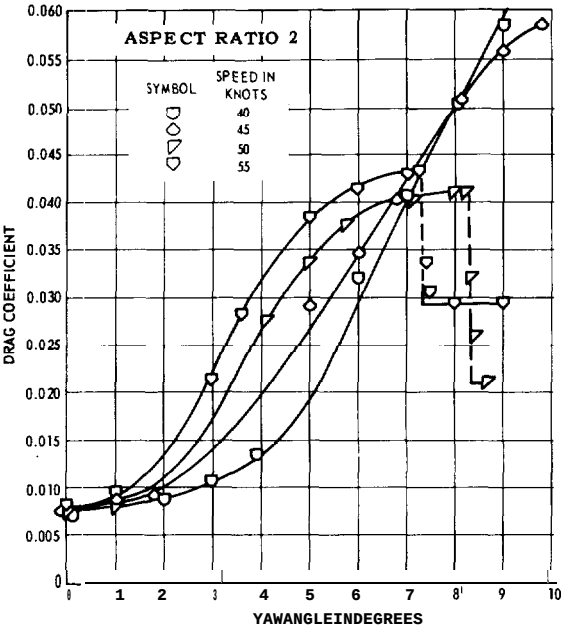

Figure 30 — Drag Coefficient versus Yaw Angle for Model 2

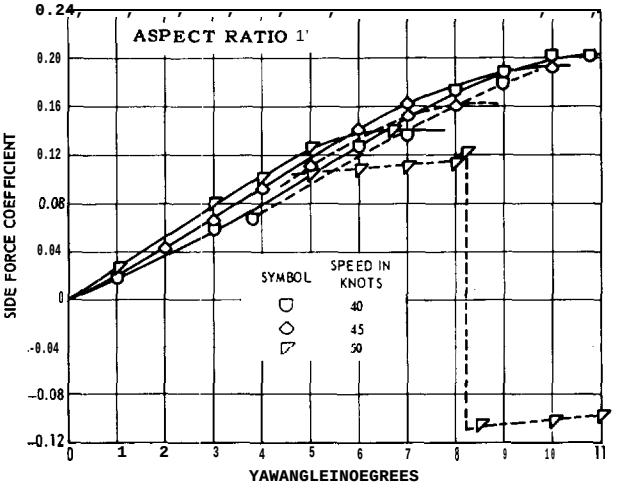

Figure 31 — Side Force Coefficient versus Yaw Angle for Models 2 and 4

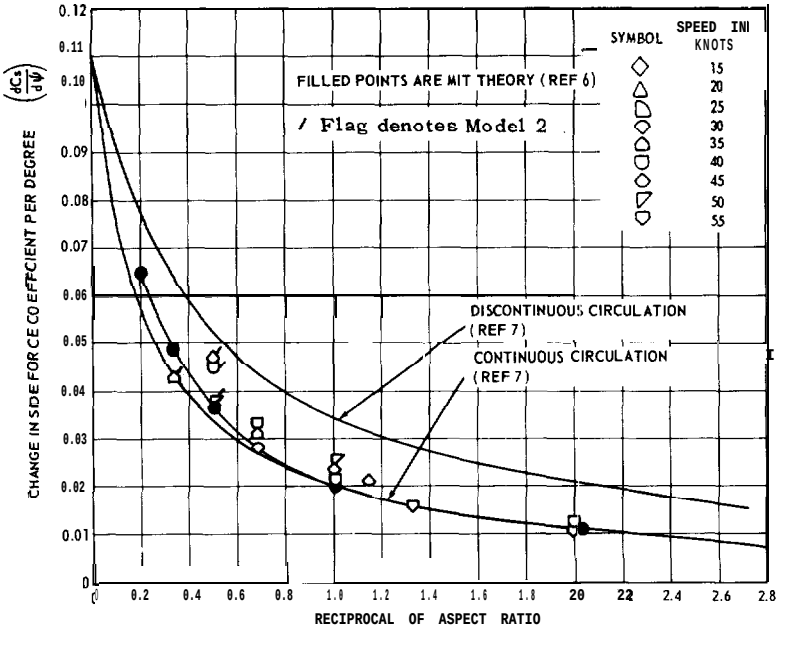

Figure 32 — Side Force Coefficient Slope versus the Reciprocal of the Aspect Ratio for Models 2 and 4

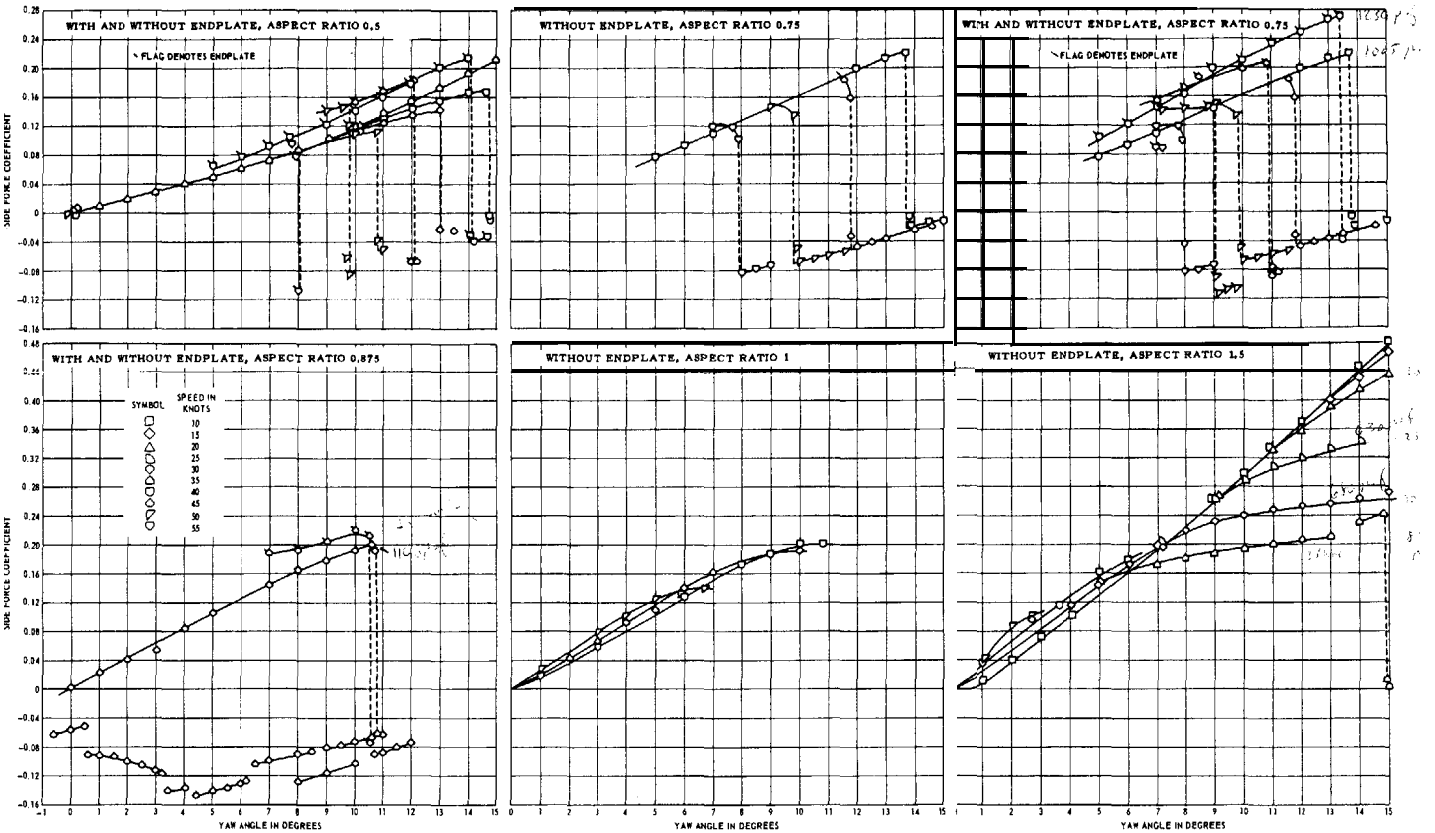

Figure 33 – Side Force Coefficient versus Yaw Angle for Model 4

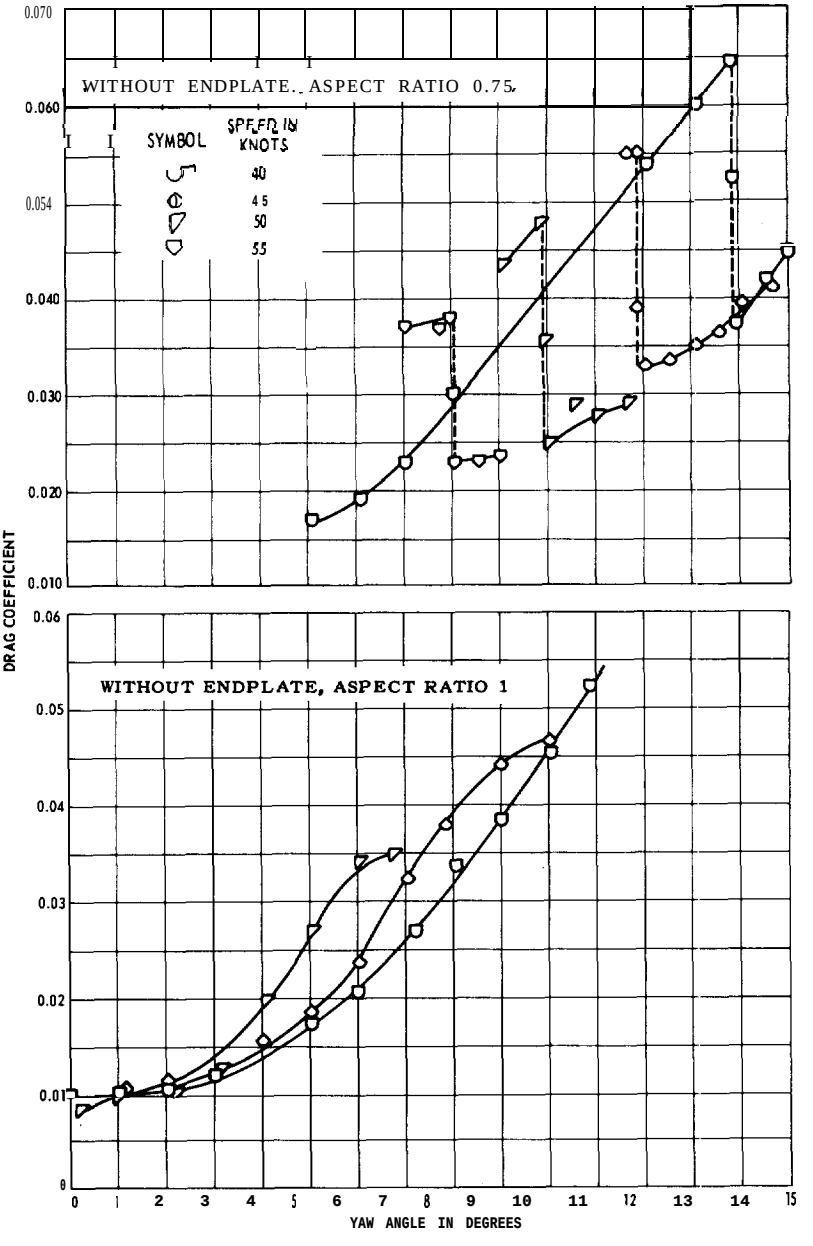

Figure 34 – Drag Coefficient versus Yaw Angle for Model 4

REFERENCES

1. Hay, A. Donald, "Flow About Semi-Submerged Cylinders of Finite Length," Princeton University (1947).

2. Breslin, J.P. and Skalak, R., "An Exploratory Study of Ventilated Flows about Yawed Surface-Piercing Struts," SIT ETT Report 668 (1957); also NASA Memo 2-23-59W (Apr 1959).

3. Waid, R.L., "Experimental Investigation of the Ventilation of Vertical Surface-Piercing Struts in the Presence of Cavitation," Lockheed Missiles and Space Company Report LMSC/0019597 (May 1968).

4. Taylor, G.I., "The Instability of Liquid Surfaces When Accelerated in a Direction Perpendicular to Their Planes," Proceedings of the Royal Society A, 201, 192-6 (1950).

5. Emmons, H.W. et al., "Taylor Instability of Finite Surface Waves," Journal of Fluid Mechanics, Vol. 7, Part 2 (Feb 1960).

6. Ashley, H. et al., "New Direction in Lifting Surface Theory," American Institute of Aeronautics and Astronautics Journal, Vol. 3, No. 1, pp. 3-16 (Jan 1965). (Presented at Aero Space Sciences Meeting, New York, N.Y., January 20-22, 1964.)

7. Breslin, J.P., "The Hydrodynamic Characteristics of Several Surface-Piercing Struts," ETT Report 597 (Jan 1956).

BIBLIOGRAPHY

1. Altmann, R. and Elata, C., "Effects of Ambient Conditions, the Giravity Field, and Struts, on Flow over Ventilated Hydrofoils," Hydronautics, Inc. Technical Report 605-l (1967).

2. Barr, R.A., "Ventilation Inception of Surface Piercing and Submerged Foils and Struts," Chapter 3 of "Hydrodynamics of Hydrofoil Craft Subcavitating Hydrofoil Systems," Hydronautics, Inc. Technical Report 463-l (Apr 1964).

3. Breslin, J.E'. and Delleur, J.W., "The Hydrodynamic Characteristics of Several Surface-Piercing Struts – Part 1 – Analysis of Drag at Zero Yaw," Stevens Institute of Technology, Experimental Towing Tank (SIT ETT) Report 596 (Jan 1956).

4. Breslin, J.E'., "The Hydrodynamic Characteristics of Several Surface-Piercing Struts – Part II – Side Force Developed in the Absence of Ventilation," SIT ETT Report 597 (Jan 1956).

5. Breslin, J.P. and Skalak, R., "An Exploratory Study of Ventilated Flows about Yawed Surface-Piercing Struts," SIT ETT Report 668 (1957); also NASA Memo 2-23-59W (Apr 1959).

6. Chey, Y. and Kowalski, T., "Interference Effects of a Submerged Hydrofoil on a Surface-Piercing Strut," Davidson Laboratory Report R936 (Jun 1963).

‘7. Coffee, C.W., Jr. and McKann, R.E., “Hydrodynamic Drag of 12- and 21-Percent Thick Surface-Piercing Struts,” NACA Technical Note 3092 (Dec 1953).

8. Dobay, G.F., “Hydrofoil Designs for Surface Ventilation -- An Experimental Analysis,” 1965 Spring Meeting, Society of Naval Architects and Marine Engineers (SNAME).

9. Elata, C., “Choking of Strut-Ventilated Foil Cavitation,” Hydronautics, Inc. Technical Report 605-2 (1967).

10. Fridsma, Gerard, “Ventilation Inception on a Surface-Piercing Dihedral Hydrofoil with Plane-Face Wedge Section,” Davidson Laboratory Report R952 (Oct 1963).

11. Hay, A.D., “Flow About Semi-Submerged Cylinders of Finite Length,” Princeton University (1947).

12. Hoerner, S.F., “Some Characteristics of Spray and Ventilation,“’ Bath Iron Works Corporation, Report BIWC TR15 (Sep 1953).

13. Hoerner, S.F., “Fluid Dynamic Drag,” published by author, Midland Park, N.J. (1965).

14. Huang, T.T., “Strut Induced Downwash,” Hydronautics, Inc. Technical Report 463-7 (Sep 1965).

15. “Hydrodynamic Characteristics of Base-Vented and Supercavitating Struts for Hydrofoil Ships,” Aeroject General Corp., Von Karman Center, Oceanics Products Division, Report 2796 (Aug 1964).

16. “Hydrofoil Handbook,” Vol. II, Gibbs and Cox (1954).

17. Kaplan, P., “Tests of Surface-Piercing Struts,” SIT ETT Report LR488 (Apr 1953).

18. Kiceniuk, Taras, “A Preliminary Experimental Study of Vertical Hydrofoils of Low Aspect Ratio Piercing a Water Surface,” California Institute of Technology (CIT) Report E-55.2 (1954).

19. Lacy, R.,. “Cavitation and Ventilation of a Rudder on a Twenty-Foot Model of a Destroyer,” Lockheed Missiles and Space Company Report LMSC/A846353 (Jun 1967).

20. Lurye, J.R., “Linearized Theory of Three-Dimensional Cavity Flow with Ventilation to the Free Surface,” TRG Report TRG-156-FR (Jun 1966).

21. Martin, M., “Choking of Strut-Ventilated Foil Cavities,” Hydronautics, Inc., Summary of Report 605-2 (1967).

22. Meijer, M.C., “An Experiment Concerning Partly Closed Cavities behind a Surface-Piercing Rod,” Hydrodynamics Laboratory, CIT Report E-110.1 (Jan 1967).

23. Perry, Bryne, “Experiments on Struts Piercing the Water Surface,” CIT Report E-55.1 (1954).

24. Ramsen, John A., "An Experimental Hydrodynamic Investigation of the Inception of Vortex Ventilation," NACA TN 3903 (1957).

25. Ransleben, G.R., Jr., "Experimental Determination of Steady and Unsteady Loads on a Surface-Piercing, Ventilated Hydrofoil," Southwest Research Institute (SWRI) Report, Project 02-1546, Phase II (Jun 1967).

26. Ransleben, G.R., Jr., "Experimental Determination of Oscillatory Lift and Moment Distribution on Surface-Piercing Flexible Hydrofoils," SWRI Report, Project 38-1028-2 TR3 (Oct 1963).

27. Rothblum, R.S. and Wilburn, G.M., "Investigation of Ventilation on Surface-Piercing Struts," NSRDC Report 217-H-01 (Jun 1967).

28. Shieba, H., "Model Experiments about the Maneuverability and Turning of Ships," First Symposium on Ship Maneuverability, David Taylor Model Basin Report 1461 (Oct 1960).

29. Schiebe, F.R. and Wetzel, J.M., "Further Studies of Ventilated Cavities on Submerged Bodies," St. Anthony Falls Hydraulic Laboratory Project Report 72 (Oct 1964).

30. Thomsen, P., "Cavity Shape and Drag in Ventilated Flow; Theory and Experiment," TRG-156-SR-2 (Feb 1963).

31. Thomsen, P., "A Comparison of Experimental Data with Simple Theoretical Results for Ventilated Flow," TRG-156-SR-1 (Aug 1962).

32. Wadlin, K.L., "Ventilated Flow with Hydrofoils," American Towing Tank Conference (ATTC) University of California, Berkeley (Sep 1959).

33. Wadlin, K.L., "Mechanics of Ventilation Inception," 2nd ONR Symposium on Naval Hydrodynamics, Government Printing Office, ACR-38 (1958), pp. 405-445.

34. Waid, R.L., "Experimental Investigation of the BUSHIPS Parent Hydrofoil – Lockheed Underwater Missile Facility," Lockheed Missiles and Space Company Report LMSC/805568 (Dec 1965).

35. Waid, R.L., "Experimental Investigations of the Ventilation of Vertical Surface-Piercing Struts in the Presence of Cavitation," Lockheed Missiles and Space Company Report LMSC/0019597 (May 1968).

36. Waid, R.L., "Cavity Flows – (part of report on cavitation)," 15 th ATTC, Ottawa, Canada (Jun 1968).

37. Wetzel, J.M., "Experimental Studies of Air Ventilation of Vertical, Semi-Submerged Bodies," St. Anthony Falls Hydraulic Laboratory Project Report 57 (Jul 1957).

38. Wetzel, J.M., "Ventilation of Bodies Piercing a Free Surface," 2nd ONR Symposium on Naval Hydrodynamics, Government Printing Office, ACR-38 (1958), pp. 447–465.

39. Wetzel, J.M. and Foerster, K.E., "Force Characteristics of Restrained Naturally Ventilated Hydrofoils in Regular Waves," St. Anthony Falls Hydraulic Laboratory Project Report 68 (Mar 1965).

40. Wilburn, G.M. and Haller, H.S., Jr., "Experimental Measurements of the Steady Lift, Drag and Moment on Surface-Piercing Struts," David Taylor Model Basin Report 1778 (Oct 1965).

41. Andrews, T.M., "Pendulum Tests of Two Cruise Foils and Various Struts," Dynamic Developments, Inc. Contract 2852(00) (Oct 1961).

42. Huang, T.T., "Experimental Study of a Low Modulus Flutter Model for Strut-Foil-Pod Configurations," Hydronautics, Inc. TR-459-2 (Jul 1967).

43. Ramsen, John A. and Vaughan, V.L., Jr., "Hydrodynamic Tares and Interference Effects for a 12-Percent Thick Surface-Piercing Strut and an Aspect-Ratio-O.25 Lifting Surface," NACA TN 3420 (Apr 1955).

INITIAL DISTRIBUTION

Copies

4 NAVSHIPSY SCOM
- 1 SHIPS 0342
- 2 SHIPS 2052
- 1 SHIPS 03412

3 ONR
- 2 Code 438
- 1 Code 41'1

1 ONR Boston

1 ONR Chicago

1 ONR New York

1 ONR Pasadena

1 ONR San Francisco

1 ONR London

3 NAVSEC
- 1 SEC 6132
- 1 SEC 6136
- 1 SEC6140

1 NAVFACENGCOM

1 SPECPROJO
Attn: Dr. John Craven (NSP-001)

1 CO NAVAIRDEVCEN

1 NASL

1 NRL (Code 2027)

1 NAVUWRES

1 NAVOCEANO

1 CDR, U.S. Naval Proving Ground
Dahlgren, Va 22448
Attn: Tech Lib

1 CIVENGRLAB Attn: Code L31

1 NAVSHIPYD BSN

1 NAVSHIPYD CHASN

1 NAVSHIPYD NORVA

1 NAVSHIPYD PHILA

1 NAVSHIPYD PTSMH

Copies

1 NAVSHIPYD BREM

1 AFFDL (FDDS -Mr. J. Olsen)
Wright-Patterson AFB, Ohio 45433

1 NASA Sci & Tech
Information Facility
P.O. Box 33
College Park, Md 20740

1 Library of Congress
Sci & Technology Div

1 COGARD
Attn: Div of Merchant Marine Safety

1 DIRECTOR, Waterways Experiment Station
Box 631
Vicksburg, Mississippi 39180
Attn: Res Center Lib

1 Univ of Bridgeport
Bridgeport, Connecticut 06602
Attn: Prof. Earl Uram
Mechanical Engr Dept

3 Naval Architecture Dept
College of Engr, Univ of California
Berkeley, Calif 94720
Attn: 1 Prof J.R. Paulling
1 Prof J.V. Wehausen
1 Dr. H.A. Schade

1 NASA Langley
Attn: Dr. E.C. Yates, Jr., MS 340

3 CIT, Pasadena
Attn: 1 Dr. A.J. Acosta
1 Dr. T.Y. Wu
1 Dr. M.S. Plesset

1 Univ of Connecticut
Box U-37, Storrs, Connecticut 06268
Attn: Prof V. Scattron
Hydraulic Res Lab

1 Cornell Univ
Graduate School of Aerospace Engr
Ithaca, New York 14850
Attn: Prof W.R. Sears

20 DDC

Copies

1 Harvard Univ
2 Divinity Ave, Cambridge, Mass 02138
Attn: Prof G. Birkhoff
Dept of Mathe

1 Univ of Illinois
College of Engr, Urbana, Illinois 61801
Attn: Dr. J.M. Robertson
Theoretical & Applied Mechanics Dept

1 The Univ of Iowa, Iowa City, Iowa 52240
Attn: Dr. Hunter Rouse

2 The State Univ of Iowa
Iowa Inst of Hydraulic Res
Iowa City, Iowa 52240
Attn: 1 Dr. L. Landweber
1 Dr. J. Kennedy

1 Kansas State Univ
Engineering Experiment Station
Seaton Hall, Manhattan, Kansas 66502
Attn: Prof. D.A. Nesmith

1 Lehigh University, Bethlehem, Pa 18015

7 MIT, Hydro Lab
Cambridge
Attn: Prof A.T. Ippen

6 MIT, Dept NAME
Attn: 1 Dr. A.H. Keil
Rm 5-226
1 Prof P. Mandel
Rm 5325
1 Prof J.R. Kerwin
Rm 5-23
1 Prof P. Leehey
Rm 5222
1 Prof M. Abkowitz
1 Dr. J.N. Newman

2 Univ of Michigan, Dept of NAME, Ann Arbor
Attn: 1 Dr. T.F. Ogilvie
1 Prof. H. Benford

5 St. Anthony Falls Hydraulic Lab, Univ of Minnesota, Mississippi River at 3rd Ave S.E., Minneapolis, Minnesota 55414
Attn: 1 Dir
1 Dr. C.S. Song
1 Mr. J.M. Killen
1 Mr. F. Schiebe
1 Mr. J.M. Wetzel

Copies

1 USNA

1 USNAVPGSCHOL, Monterey

1 New York Univ
Univ Heights, Bronx, New York 10453
Attn: Prof W.J. Pierson, Jr.

2 New York Univ
Courant Inst of Mathe Sci
251 Mercier St, New York, N.Y. 10012
Attn: 1 Prof A.S. Peters
1 Prof J.J. Stoker

1 Univ of Notre Dame, Notre Dame, Indiana 46556
Attn: Dr. A.F. Strandhagen

2 The Pennsylvania State Univ
Ordnance Res Lab, Univ Park, Pa 16801
Attn: 1 Director
1 Dr. G. Wislicenus

3 Stanford Univ, Stanford, Calif 94305
Attn: 1 Prof H. Ashley, Dept of Aeronautics & Astronautics
1 Prof R.L. Street, Dept of Civil Engr
1 Prof B. Perry, Dept of Civil Engr

3 SIT, DL Attn: Dr. J. Breslin

1 Worcester Polytechnic Inst
Alden Res Labs
Worcester, Mass 01609
Attn: Director

1 Aerojet-General Corp
1100 W. Hollyvale St, Azusa, Calif 91702
Attn: Mr. J. Levy,, Bldg 160, Dept 4223

1 Bethlehem Steel Corp
Central Technical Div
Sparrows Point Yard, Sparrows Point, Md 21219
Attn: Mr. A.D. Hoff, Technical Manager

1 Bethlehem Steel Corp
25 Broadway, New York, N.Y. 10004
Attn: Mr. H. DeLuce

1 Cornell Aeronautical Lab
Applied Mechanics Dept, P.O. Box 235
Buffalo, New York 14221
Attn: Dr. I.C. Statler

Copies

6 The Boeing Co, Aerospace Grp
Advanced Marine Systems
P.O. Box 3707
Seattle, Washington 98124
Attn: 1 Mr. H. French
1 Mr. R. Hatte
1 Mr. R. Hubard
1 Mr. F.B. Watson
1 Mr. W.S. Rowe
1 Mr. T.G.B. Marvin

1 Electric Boat Div, General Dynamics Corp
Groton, Connecticut 06340
Attn: Mr. V.T. Boatwright, Jr.

1 General Applied Sci Labs, Inc.
Merrick & Stewart Avenues
Westbury, L.I., N.Y. 11590
Attn: Dr. F. Lane

1 Gibbs & Cox, Inc.
21 West Street
New York, N.Y. 10006

1 Grumman Aircraft Engr Corp
Bethpage, L.I., N.Y. 11714
Attn: Mr. W.P. Carl

2 Hydronautics, Incorporated
Pindell School Road
Howard County
Laurel, Md 20810
Attn: 1 Mr. P. Eisenberg
1 Mr. M.P. Tulin

1 Nat'l Sci Foundation
Engr Division
1800 G. Street, N.W.
Washington, D.C. 20550
Attn: Director

1 Newport News Shipbuilding & Drydock Co
4101 Washington Ave
Newport News, Va 23607

1 Oceanics, Incorporated
Technical Industrial Park
Plainview, L.I.
New York 11803
Attn: Dr. Paul Kaplan

Copies

1 Robert Taggart, Inc.
3930 Walnut Street
Fairfax, Va 22030
Attn: Mr. R. Taggart

1 Sperry-Piedmont Co
Charlottesville, Va 22901
Attn: Mr. T. Noble

UNCLASSIFIED

Security Classification

DOCUMENT CONTROL DATA - R & D

(Security classification of title, body of abstract and indexing annotation must be entered when the overall report is classified)

1 ORIGINATING ACTIVITY *(Corporate author)*

Naval Ship Research and Development Center
Washington, D. C. 20007

2a. REPORT SECURITY CLASSIFICATION

UNCLASSIFIED

2b. GROUP

3 REPORT TITLE

VENTILATION, CAVITATIOS AND OTHER CHARACTERISTICS OF HIGH SPEED SURFACE PIERCING STRUTS

4. DESCRIPTIVE NOTES *(Type of report and inclusive dates)*

Final Report for work performed from November 1966 to January 1968

5AU THOR(S) *(First name, middle initial, last name)*

Richard S. Rothblum, Dennis A. Mayer, and Gene M. Wilburn

6. REPORT DATE	7a. TOTAL NO. OF PAGES	7b. NO. OF REFS
July 1969	48	7

8a. CONTRACT OR GRANT NO.	9a. ORIGINATOR'S REPORT NUMBER(S)
5. PROJECT NO. Subproject S4606X Task 1703	3023
c.	9b. OTHER REPORT NO(S) *(Any other numbers that may be assigned this report)*
d.	

10. DISTRIBUTION STATEMENT

This document is subject to special export controls and each transmittal to foreign governments or foreign nationals may be made only with prior approval of Naval Ship Research and Development Center, Code 500.

11 SUPPLEMENTARY NOTES	12. SPONSORING MILITARY ACTIVITY
	Naval Ship Systems Command Washington, D. C.

13. ABSTRACT

A family of five struts was towed to pierce the water surface vertically in the high-speed towing tank of the Naval Ship Research and Development Center. The purpose of the tests was to determine the effect of speed and certain geometric parameters on the ventilation, cavitation, and other characteristics of surface-piercing struts.

It was found that upon ventilation of high speeds, significant reversals of side force may occur on surface-piercing struts. For initially undisturbed conditions, ventilation at high speeds is more likely to occur on blunt-nosed struts. Cavitation results in unpredictable, nonlinear, and highly unsteady force coefficients. Mean force coefficients are presented for the conditions tested. There was some indication that modeling of ventilation inception conditions may be accomplished if Froude and cavitation number are scaled.

DD FORM 1 NOV 65 1473 (PAGE 1)

S/N 0101-807-6801

UNCLASSIFIED

Security Classification

14. KEY WORDS	LINK A ROLE	LINK A WT	LINK B ROLE	LINK B WT		WT
Surface piercing struts						
Hydrofoil struts						
Ventilation						
Cavitation						
Lift forces on struts						
Forces on struts						
Drag forces on struts						
Side forces on struts						

Naval Ship Research and Development Center. Report 3023.
VENTILATION, CAVITATION AND OTHER CHARACTERISTICS OF HIGH SPEED SURFACE PIERCING STRUTS, by Richard S. Rothblum, Dennis A. Mayer, and Gene M. Wilbum. July 1969. iv. 44p. illus., refs. UNCLASSIFIED

A family of five struts was towed to pierce the water surface vertically in the high-speed towing tank of the Naval Ship Research and Development Center. The purpose of the tests was to determine the effect of speed and certain geometric parameters on the ventilation, cavitation, and other characteristics of surface-piercing struts.

It was found that upon ventilation of high speeds, significant reversals of side force may occur on surface-piercing struts. For initially undisturbed conditions, ventilation at high speeds is more likely to occur on blunt-nosed struts. Cavitation results in

1. Surface-piercing struts--Ventilation--Measurement
2. Surface-piercing struts--Ventilation--Force effects
3. Surface-piercing struts--Cavitation--Measurement
4. Surface-piercing struts--Cavitation--Force effects
5. Model basins--NSRDC--High Speed Towing Tank

I. Rothblum, Richard S.
II. Mayer, Dennis A.
III. Wilburn, Gene M.

Naval Ship Research and Development Center. Report 3023.
VENTILATION, CAVITATION AND OTHER CHARACTERISTICS OF HIGH SPEED SURFACE PIERCING STRUTS, by Richard S. Rothblum, Dennis A. Mayer, and Gene M. Wilburn. July 1969. iv, 44p. illus., refs. UNCLASSIFIED

A familv of five struts was towed to pierce the water surface vertically-in the high-speed towing tank of the Naval Ship Research and Development Center. The purpose of the tests was to determine the effect of speed and certain geometric parameters on the ventilation, cavitation, and other characteristics of surface-piercing struts.

It was found that upon ventilation of high speeds, significant reversals of side force may occur on surface-piercing struts. For initially undisturbed conditions, ventilation at high speeds is more likely to occur on bluntnosed struts. Cavitation results in

1. Surface-piercing struts--Ventilation--Measurement
2. Surface-piercing struts--Ventilation--Force effects
3. Surface-piercing struts--Cavitation--Measurement
4. Surface-piercing struts--Cavitation--Force effects
5. Model basins--NSRDC--High Speed Towing Tank

I. Rothblum, Richard S.
II. Mayer, Dennis A.
III. Wilburn, Gene M.

Naval Ship Research and Development Center. Report 3023.
VENTILATION, CAVITATION AND OTHER CHARACTERISTICS OF HIGH SPEED SURFACE PIERCING STRUTS, by Richard S. Rothblum, Dennis A. Mayer, and Gene M. Wilburn. July 1969. iv, 44p. illus., refs. UNCLASSIFIED

A family of five struts was towed to pierce the water surface vertically in the high-speed towing tank of the Naval Ship Research and Development Center. The purpose of the tests was to determine the effect of speed and certain geometric parameters on the ventilation, cavitation, and other characteristics of surface-piercing struts.

It was found that upon ventilation of high speeds, significant reversals of side force may occur on surface-piercing struts. For initially undisturbed conditions, ventilation at high speeds is more likely to occur on blunt-nosed struts. Cavitation results in

1. Surface-piercing struts--Ventilation--Measurement
2. Surface-piercing struts--Ventilation--Force effects
3. Surface-piercing struts--Cavitation--Measurement
4. Surface-piercing struts--Cavitation--Force effects
5. Model basins--NSRDC--High Speed Towing Tank

I. Rothblum, Richard S.
II. Mayer, Dennis A.
III. Wilbum, Gene M.

Naval Ship Research ond Development Center. Report 3023.
VENTILATION, CAVITATION AND OTHER CHARACTERISTICS OF HIGH SPEED SURFACE PIERCING STRUTS, by Richard S. Rothblum, Dennis A. Mayer, and Gene M. Wilburn. July 1969. iv, 44p. illus., refs. UNCLASSIFIED

A family of five struts was towed to pierce the water surface vertically in the high-speed towing tank of the Naval Ship Research and Development Center. The purpose of the tests was to determine the effect of speed and certain geometric parameters on the ventilation, cavitation, and other characteristics of surface-piercing struts.

It was found that upon ventilation of high speeds, significant reversals of side force may occur on surface-piercing struts. For initially undisturbed conditions, ventilation at high speeds is more likely to occur on bluntnosed struts. Cavitation results in

1. Surface-piercing struts--Ventilation--Measurement
2. Surface-piercing struts--Ventilation--Force effects
3. Surface-piercing struts--Cavitation-Measurement
4. Surface-piercing struts--Cavitation--Force effects
5. Model basins--NSRDC--High Speed Towing Tank

I. Rothblum, Richard S.
II. Mayer, Dennis A.
III. Wilbum, Gene M.

unpredictable, nonlinear, and highly unsteady force coefficients. Mean force coefficients are presented for the conditions tested. There was some indication that mddeling of ventilation inception conditions may be accomplished if Froude and cavitation number are scaled.

unpredictable, nonlinear, and highly unsteady force coefficients. Mean force coefficients are presented for the conditions tested. There was some indication that mddeling of ventilation inception conditions may be accomplished if Froude and cavitation number are scaled.

unpredictable, nonlinear, and highly unsteady force coefficients. Mean force coefficients are presented for the conditions tested. There was some indication that modeling of ventilation inception conditions may be accomplished if Froude and cavitation number are scaled.

unpredictable, nonlinear, and highly unsteady force coefficients. Mean force coefficients are presented for the conditions tested. There was some indication that mddeling of ventilation inception conditions may be accomplished if Froude and cavitation number are scaled.